2005

Photobiological and thermal effects of UVA light on cell culture

Julianne Forman
Louisiana State University and Agricultural and Mechanical College, jforma1@lsu.edu

PHOTOBIOLOGICAL AND THERMAL EFFECTS OF UVA LIGHT ON CELL CULTURE

A Thesis

Submitted to the Graduate Faculty of the
Louisiana State University and
Agricultural and Mechanical College
In partial fulfillment of the
Requirements for the degree of
Master of Science in Biological and Agricultural Engineering

In

The Department of Biological and Agricultural Engineering

by
Julianne Forman
B.S., Louisiana State University, 2002
December 2005

Acknowledgements

I would like to thank my major advisor, Dr. Todd Monroe, for his guidance, suggestions, knowledge, and assistance. His patience and support helped me to make this possible, and I really appreciate his allowing me the opportunity to work in the lab, even at a time when the number of graduate students in the lab was near capacity. I would also like to express appreciation to Dr. Marybeth Lima for the years of guidance and mentoring during my undergraduate work, which helped me to get to get to this point in my degree. I also express gratitude to Dr. Mandi Lopez for serving on my committee and offering me her advice and assistance. Additionally, special thanks go to Marilyn Dietrich in the flow cytometry core at Veterinary Medicine for her help, suggestions, and use of the flow cytometer.

This material is based upon work supported under a National Science Foundation Graduate Research Fellowship, which provided me with financial support. I would also like to thank Dr. Daniel Thomas for allowing me to be a part of the department and the various people in the Biological Engineering Department who have assisted me during my master's work. I would also like to acknowledge my fellow students, Rick Blidner, Bilal Ghosn, Carla Haslauer, Mindi Huguet, Michelle Urbina, and Daisy Dong, and the work of undergraduate students, Meredith Lapre, Christopher Kennedy, Sarah DeLeo, Josh Reaves, and John Casey.

Finally, I am grateful for my family and friends who supported me when I needed it most. I especially would like to thank my parents and my sister for their guidance and motivation during my graduate school adventure. And last but not least, I would like to thank Bryan Audiffred for his constant support, encouragement, and assistance throughout the pursuit of my degree.

Table of Contents

Acknowledgements ii

List of Tables v

List of Figures vi

List of Abbreviations viii

Abstract x

Chapter 1 Background and Introduction 1
- Photoactivation 1
- Published Results of DMNPE Photoactivation in HeLa Cells 2
- UV Light Interactions with Biology 4
  - Non-Apoptotic Effects 4
- Apoptosis 5
  - Annexin V Apoptosis Assay 6
- UV-Induced Apoptosis 8
- Overview of UVA-Induced Apoptosis Studies 8
- Overview of UVB-Induced Apoptosis Studies 9
- UVA Dose and Mode of Exposure Compared to Prior Works 10
- Thermal Effects Associated with UVA Photoactivation 11
- Research Significance and Project Objectives 15

Chapter 2 Quantitative Effects of 365nm Photoactivating Light on HeLa Cells 16
- Introduction 16
- Materials and Methods 18
  - Methods Overview 18
  - Materials 19
  - Cell Culture 19
  - UVA Light Source Characterization 19
  - Photoexposure Protocol 21
  - Temperature Control System 21
  - Temperature Effects Protocol 23
  - UVB Irradiation 23
  - Brightfield Phase-Contrast Microscopy 23
  - Annexin V-Cy5/PI Apoptosis Assay and Analysis 23
  - Statistical Analysis 24
- Results 24
  - Thermal Effects of Light Exposure 24
  - UVA Cell Damage Assessed by Microscopy of Adherent Cells 25
  - UVA Cell Damage Assessed by Flow Cytometry 26
  - Importance of Cell Confluence for Cell Health 28
  - Dose-Response for the GreenSpot and BlakRay 30

Modeling Dose-Response of GS and BR....31
Effect of Cooling on Photoactivation....33
Photoduration Effects....33
Discussion....34

Chapter 3 Conclusions and Future Considerations....37
Conclusions....37
Future Considerations....39

References....42

Appendix A: Annexin V-Cy5, PI Apoptosis Assay Protocol....46

Appendix B: Basic Stamp Program for Thermocouple Kit....47

Appendix C: Programmable Logic Control: Pulsed GreenSpot....52

Appendix D: Staurosporine Dose, Post-Exposure Time....53

Vita....54

List of Tables

Table 1.1 UVA-Induced Apoptosis Review 12

Table 1.2 UVB-Induced Apoptosis Review 13

List of Figures

1.1 DMNPE-cage molecule is released upon photolysis with 365nm UV light..... 2

1.2 Strategy for light-activated gene expression in cultured cells 2

1.3 Effects of 365nm light doses on caged and native pGFP expression 3

1.4 Cartoon of the annexin V-Cy5, propidium iodide assay..... 7

1.5 Apoptosis cascade of events after UV exposure is shown..... 8

2.1 Light source spectral characterization 20

2.2 Control and measurement system for light-induced thermal effects 21

2.3 The BlakRay light source and peltier-driven cold plate with temperature controller are shown 22

2.4 Temperature increase due to UVA light sources 25

2.5 Phase-contrast images (40X and 10X) of (a) Live, (b) Dead, and (c) UVA-treated (10.74 J/cm^2) HeLa cells.....26

2.6 Qualitative cytometer scatterplot comparison among treatments.....27

2.7 Qualitative cytometer fluorescence dotplot comparison among treatments.....28

2.8 Effect of cell density on annexin V apoptosis assay protocol 29

2.9 Dose-response for the GreenSpot with different cell seeding densities 30

2.10 Dose-response of UVA light sources.....31

2.11 Modeling GreenSpot dose-response 32

2.12 Modeling BlakRay dose-response 32

2.13 Effect of cooling-assisted photoactivation for the BlakRay (BR) (5.37 J/cm^2) and GreenSpot (GS) (14.31 J/cm^2) UVA light sources 33

2.14 Various doses and durations of photoexposure of GS and BR explored the effect of duration of exposure on cell viability.....34

3.1 Effect of photoduration on cell viability.....40

A.C.1 GreenSpot PLC wiring diagram.....52

A.D.1 Staurosporine dosing, post-exposure timing.....53

List of Abbreviations

AO	acridine orange
ATP	adenosine triphosphate
BR	BlakRay B100-AP light source
cAMP	cyclic adenosine monophosphate
DMEM-RS	Dulbecco's Modified Eagle's Medium-Reduced Serum
DMNPE	1-(4,5-dimethoxy-2-nitrophenyl) diazoethane
DNA	deoxyribonucleic acid
EB	ethidium bromide
ELISA	enzyme-linked immunosorbent assay
FACS	fluorescence activated cell sorting
FBS	fetal bovine serum
FITC	fluorescein
GFP	green fluorescent protein
GS	GreenSpot light source
GSH	glutathione
HaCaT	human keratinocyte cell line
HeLa	human epithelial carcinoma cells
HMC-1	human mast cell line
HO-1	heme-oxygenase-1
Hsp	heat shock protein
IP_3	inositol triphosphate
IR	infrared

PARP	Poly (ADP-ribose) polymerase
PI	propidium iodide
PLC	programmable logic control
PS	phosphatidylserine
PTC	positive temperature coefficient
ROS	reactive oxygen species
SCL-A431	skin-derived squamous-cell carcinoma cell line
STR	staurosporine
TUNEL	terminal deoxynucleotidyl transferase dUTP nick end labeling
UV	ultraviolet
UVA	320-400nm ultraviolet
UVB	290-320nm ultraviolet
UVC	200-290nm ultraviolet
YO-PRO-1	monomeric cyanine nucleic acid stain (491/509)

Abstract

The objective of this study is to characterize the photobiological and thermal effects of UVA light on cell cultures. While near-ultraviolet light has been widely used to photoactivate fluorophores and caged compounds in cells, little is known of the long-term biological effects of this light. UVA (320-400nm) photoactivating light has been used for studying fast kinetic processes and is now being employed in higher doses to target longer duration phenomena (e.g. gene expression and silencing). Photoexposure experiments using 365nm light will examine how longer duration and increased UV doses affect photoactivation cell studies.

Apoptotic and cellular injury assays have been used to determine the nature and threshold of this light-induced effect. UVA light sources of low and high intensity have been used for light doses up to 23.85 J/cm^2. HeLa cells exposed to staurosporine, high intensity UVA, and equivalent UVB served as positive UVA-induced and UVB-induced apoptotic controls. Cells were stained with annexin V-Cy5 and propidium iodide for apoptosis analysis with a conventional flow cytometer. Cell cultures at lower densities had higher percentages of apoptotic and dead cells, and were also more susceptible to UVA damage than more dense cell seedings. The dose to induce apoptosis and death in 50% of the cells ($dose_{1/2}$) was determined for two different commercially available UVA light sources: 7.6 J/cm^2 for the GreenSpot photocuring system and 2.52 J/cm^2 for the BlakRay lamp. No significant cellular responses were found for doses below 1.6 J/cm^2 from the GreenSpot light source. A temperature control and measurement system was used to determine direct heating from the UVA sources and also the effect that cooling culture dishes has on minimizing cell damage. Photoduration was also found to be significant in determining UVA photoactivation doses. Together, these results show that many of these parameters are important for optimizing photobiological studies.

Chapter 1

Background and Introduction

Photoactivation

UVA light (320-400nm) is commonly used in molecular methods of photoactivation. Photoactivation is a technique that uses light to convert an inert molecule into an active state, such as converting a non-fluorescent molecule into a fluorescent probe that can be tracked in living cells. The ability to temporally and spatially control photoactivatable proteins has resulted in their wide use to study protein behavior in living cells. Photobleaching is another light-dependent technique in which a high-intensity laser extinguishes (photobleaches) fluorescence in a very specific selected region and allows for monitoring the recovery of fluorescence over time (Lippincott-Schwartz, Altan-Bonnet et al., 2003). Photoactivation is also commonly used in the ultraviolet (UV)-light-induced release of a caged group from a "caged" compound.

Caged compounds have a covalently attached group which acts to repress bioactivity of the target molecule (Kaplan, Forbush et al., 1978). Upon light exposure, photolysis releases the cage and restores activity. This technique has allowed the study of many rapid biochemical processes whereby inert caged material can be loaded into cells or tissues and released rapidly with a pulse of light. This is advantageous over diffusing in large concentrations of an active metabolite, which can make kinetic analysis difficult. Caged compounds have traditionally been small compounds such as neurotransmitters, second messengers, amino acids, and nucleotides. The classic example is DMNPE-caged ATP shown in Figure 1.1. ATP is released from 365nm light exposure that photocleaves the cage group. Caged chemistries are now being used to control activities of large biomolecules, such as proteins and nucleic acids, which require more attached cages per target molecule, necessitating increased light doses to achieve more efficient

uncaging. Based on previous studies with DMNPE-caged ATP, DMNPE (1-(4,5-dimethoxy-2-nitrophenyl)diazoethane) is the molecule also used to cage DNA.

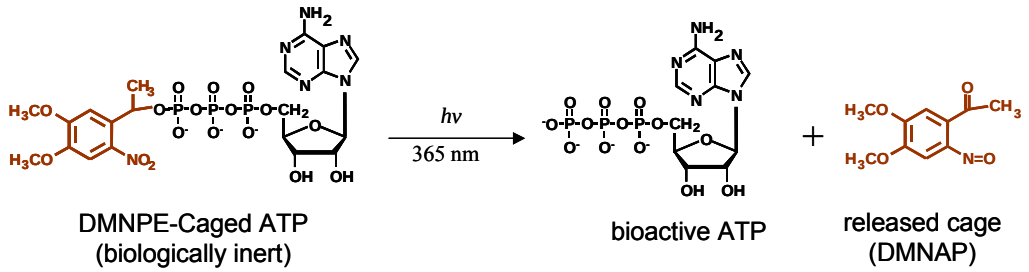

Figure 1.1 DMNPE-cage molecule is released upon photolysis with 365nm UV light.

Published Results of DMNPE Photoactivation in HeLa Cells

The caging method to control DNA bioactivity has shown promise when the DMNPE-caged DNA technique was applied to living cells (Monroe, McQuain et al., 1999). Caged plasmids coding for green fluorescent protein (GFP) were liposome-transfected into HeLa (human epithelial carcinoma) cell cultures (Figure 1.2). Selected samples were exposed to varying doses of light (0-5.6 J/cm^2) from the same light source. Following cell harvesting (48 hours), GFP expression was assessed using flow cytometry. These previous studies have shown that there is a significant increase in GFP expression when caged samples are exposed to 0.25 J/cm^2 light

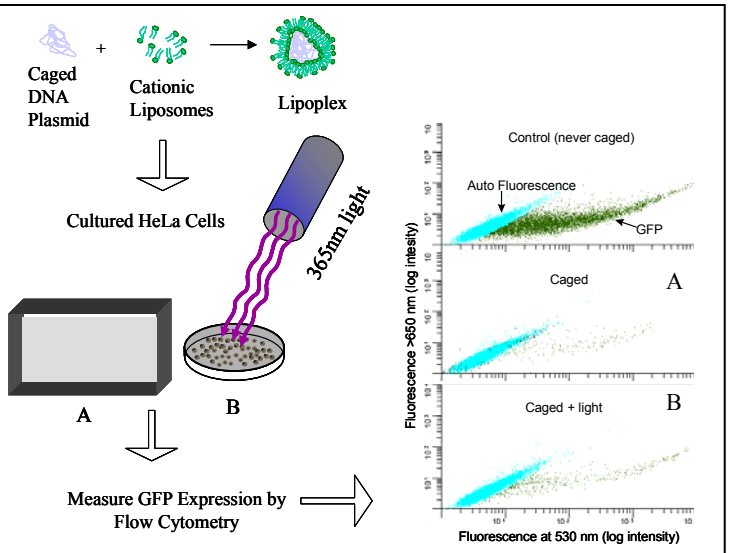

Figure 1.2 Strategy for light-activated gene expression in cultured cells. Using liposomal techniques, cells are transfected with caged plasmids, and selected cultures (A) are held in the dark, while others (B) are exposed to light. Expression of caged (A) vs. caged+light (B) cultures are measured using flow cytometry.

(Fig. 1.2). GFP-positive cells are expressed with respect to the control. Once caged, there is a low level (25.8 ±3%) of GFP expression. Exposure to light (flashing) doubles the level of expression. The data is expressed as a fraction of positive control cells (cells transfected with native, non-caged GFP plasmids). This was done because the efficiency of liposomal transfection varied based on the confluency and cell cycle of the cells, which was not confined for these experiments.

HeLa cells, transfected with native (non-caged) plasmids and subjected to increasing 365nm light doses, were observed to have a decrease in expression as light exposure doses were increased (Fig. 1.3). Two explanations were proposed for the decrease in GFP expression, either physical damage to the actual DNA plasmids or a cellular response to light-induced injury.

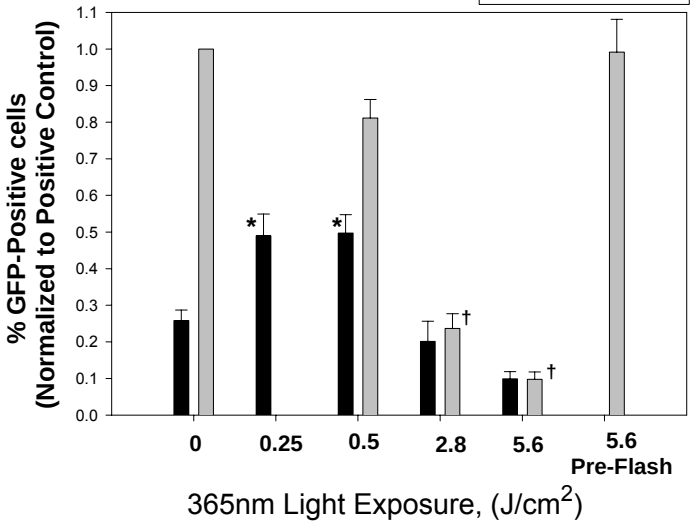

Figure 1.3 Effects of 365nm light doses on caged and native pGFP expression in HeLa cells (Monroe, McQuain et al., 1999).

In order to see if the DNA plasmids were being physically damaged by the light, native plasmids were exposed (*prior* to transfection) to the highest dose in these experiments, and the expression level was found to be equal to those samples receiving no light after transfection as shown in Figure 1.3. Therefore, it has been hypothesized that the decrease in GFP expression is a result of some at the time unknown cellular response, rather than direct plasmid DNA damage. 365nm falls into the UVA (320-400 nm) category and is thought to be far less damaging to cells than UVB (290-320 nm) and UVC (200-290 nm) ultraviolet light. In order for this caging

chemistry technique to be successful in targeting genetic activities, the photoactivation process must not harm the cells.

UV Light Interactions with Biology

Ultraviolet (UV) radiation consists of three ranges: UVA (320-400 nm), UVB (290-320 nm), and UVC (200-290 nm). Ultraviolet radiation affects various molecular targets of the cell including DNA, cell surface receptors, kinases, phosphatases, and transcription factors (Kulms and Schwarz 2002). The biological effects of UV radiation occur when a cellular chromophore absorbs and transduces the energy into a biochemical signal. Responses include but are not limited to the release of mediators, altered surface receptors, and induction of apoptosis, or programmed cell death (Kulms, Poppelmann et al., 2000).

UVA light is used for photoactivation of the DMNPE cage molecule described previously. While UVA doesn't possess the high energy of UVC light, it has been shown in high doses to cause apoptosis in biological tissues. Little is known about the molecular mechanism involved in UVA-induced apoptosis. It has been proposed that the initiation of biological effects of UVA radiation involves the absorption by a non-DNA chromophore, which causes the generation of active oxygen species or upregulation of critical target molecules (Tyrrell and Keyse 1990).

Non-Apoptotic Effects

UVA effects have been reported to induce actin cytoskeleton damage (Villanueva, Vidania et al., 2000). UVA exposure of 3T3 mouse fibroblasts and V79 Chinese hamster fibroblasts caused disintegration of actin microfilaments and formation of multinucleated cells (Brathen, Banrud et al., 2000). The relationship between UVA-induced oxidative stress and apoptosis has been reported in literature. UVA damage was found to depend very strongly on the presence of oxygen. The formation of Reactive Oxygen Species (ROS) affects cellular

effects, including glutathione (GSH) content depletion, lipid peroxidation, and induction of heme-oxygenase-1 (HO-1) (Pourzand and Tyrrell 1999).

Apoptosis

Apoptosis is a crucial cellular mechanism for maintaining tissue homeostasis, natural defense mechanisms, and the aging process. Inappropriate regulation of apoptosis results in disease. For therapeutic intervention, a clear understanding and ability to detect and control apoptotic events is important. Apoptosis is characterized by significant changes in the cell membrane and nucleus.

Apoptotic morphological events include condensed chromatin, cell shrinkage and blebbing, asymmetry of the plasma membrane, and formation of apoptotic bodies, which are phagocytized without causing inflammation (Kerr, Wyllie et al., 1972). Along with nucleus fragmentation, a biochemical hallmark of apoptotic cells includes the cleavage of DNA into approximately 200 base pair fragments, which are resolved into a "DNA ladder" by electrophoresis (Willingham 1999). The morphological changes result from characteristic molecular and biochemical events, such as the activation of caspases and release of cytochrome c.

There are two distinct forms of cell death. Necrosis is an uncontrollable pathological form of cell death, characterized by cell swelling, plasma membrane rupture, and inflammation. It is a result of chemical or physical damage to the cell. Apoptosis is triggered by milder environmentally damaging stimuli, such as ultraviolet radiation or lack of growth factors. Loss of cell membrane integrity is a very late event during apoptosis and is similar to the compromised cell membrane characteristic of necrosis. Dissimilar morphological and biochemical features are used to differentiate between necrosis and apoptosis.

Early apoptotic cells are recognized by morphological changes that begin with condensing chromatin, cell shrinkage, and loss of asymmetry of the plasma membrane (Kerr, Wyllie et al., 1972). Later apoptotic events include nucleus fragmentation, DNA "laddering," membrane blebbing, and cell fragmentation. Apoptotic bodies are small, compact vesicles that contain cytosol, condensed chromatin, and organelles. Macrophages engulf and remove apoptotic bodies from the tissues without inacting an inflammatory response. These morphological changes, characteristic of apoptotis, result from a molecular cascade of events, such as the release of cytochrome c and activation of caspases. Many apoptosis detection methods target these particular cellular events.

Apoptosis is also characterized by phosphatidylserine (PS) translocation from the inner leaflet to the outer leaflet of the phospholipid bilayer, while the cell membrane remains intact. The loss of plasma membrane asymmetry is an early apoptotic event, independent of cell type (van Engeland, Nieland et al., 1998). PS exposure on the cell surface continues until the final stages of apoptosis when the cell has divided into apoptotic bodies.

Annexin V Apoptosis Assay

Early apoptosis assays relied upon morphologic changes detected by light microscopy, electron microscopy, or flow cytometry using nuclear staining dyes (Koopman, Reutelingsperger et al., 1994). Quantifying apoptosis by microscopy was inexact, and the nonvital dyes would only stain late apoptotic cells once the membrane was damaged. In 1994, Koopman and colleagues were the first to use labeled annexin V for flow cytometric detection of phosphatidylserine translocation on B cells (Koopman, Reutelingsperger et al., 1994). Ethidium bromide, a nonvital stain, was used to label necrotic cells. The binding of annexin V was found to correlate with apoptotic morphology.

The biotinylated annexin V assay has been used successfully for flow cytometric analysis of apoptosis (vanEngeland, Ramaekers et al., 1996; Chan, Luedke et al., 2003). Annexin V is a calcium-dependent, phospholipid binding protein with a high affinity for PS (vanEngeland, Ramaekers et al., 1996). By double-labeling for annexin V and either a membrane impermeable DNA stain (propidium iodide) or esterase live stain (calcein AM), distinct populations of live, apoptotic, and necrotic cells can be quantified using flow cytometric techniques (Figure 1.4). Stained cells can be viewed for qualitative results under a fluorescence microscope, using appropriate filters, and quantified by flow cytometry.

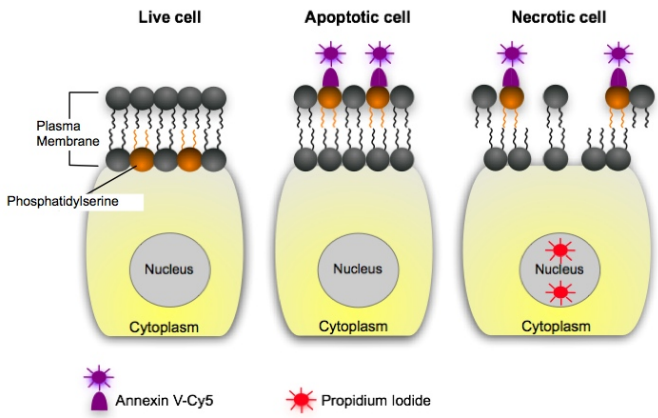

Figure 1.4 Cartoon of the annexin V-Cy5, propidium iodide assay shows the staining of live, apoptotic, and necrotic cells using annexin V binding and membrane impermeable DNA staining.

Other existing apoptosis methods are based on changes in DNA strand breaks (TUNEL assay), DNA fragmentation (DNA laddering), chromatin condensation (light microscopy examination), and alteration of membrane integrity (trypan blue or propidium iodide exclusion assays). DNA laddering, morphological examination, and exclusion assays do not allow precise quantification of apoptotic cells on a cell-by-cell basis, and the TUNEL assay can be labor-intensive and time-consuming (Leite, Quinta-Costa et al., 1999).

The labeled annexin V technique is important for early detection, as PS exposure has been found to occur at least as early as chromatin condensation (Koopman, Reutelingsperger et al., 1994). Labeled (FITC or biotin) annexin V-affinity assay allows for simultaneous labeling of other cell-surface antigens and can be analyzed quantitatively by flow cytometry and qualitatively by fluorescence microscopy.

UV-Induced Apoptosis

Apoptosis can be triggered by exposure to UV radiation (Godar 1999). Apoptosis is an important cellular defense mechanism in protecting against UV damage. An overview of the apoptotic cascade of events after UV exposure, showing the initial cell death signals (CD95, Fas) and DNA damage, is shown in Fig. 1.5. Bcl-2 (death-suppressing proto-oncogene) regulated by Bax (death promoting protein) is an important protein in UV-induced apoptosis (Kulms, Poppelmann et al., 1999). Apoptosis is detected using light and fluorescence microscopy (morphological changes) and apoptotic assays based on differential fluorescent dye-uptake quantified with flow cytometry.

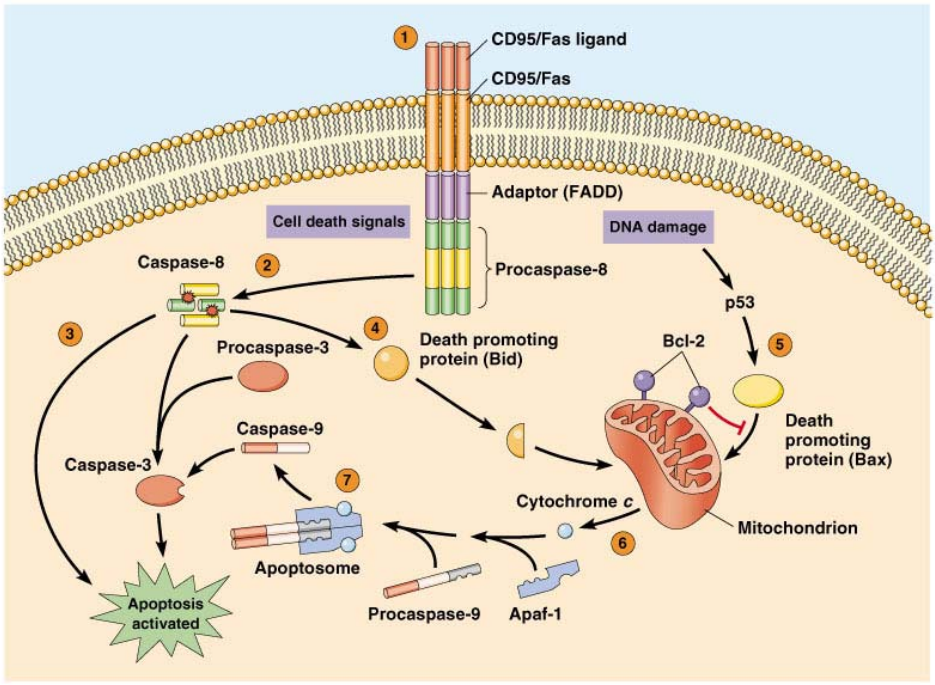

Figure 1.5 Apoptosis cascade of events after UV exposure is shown, including surface receptors and DNA damage (Becker, Kleinsmith et al., 2003).

Overview of UVA-Induced Apoptosis Studies

Previous work has demonstrated that UVA radiation initiates apoptosis by singlet-oxygen damage to the mitochondrial membrane (Godar 1999). UVA irradiation induces apoptosis within 6 hours and results in complete cell death within 24 hours (Breuckmann, von Kobyletzki

et al., 2003). This literature review consists of two tables summarizing previous research on UVA and UVB-induced apoptosis.

The UVA table created from 5 different studies summarizes parameters used in the UV-induced apoptosis (Table 1.1). Based on four of the studies in the UVA table, the UVA doses range from 2.5 to 96 J/cm^2, and the post-exposure time ranges from 3 to 72 hours. While Yao and Wang (2002) are included in the table, the UVA 0.00365 J/cm^2 dose (2 hour exposure and 2 hour post-exposure time) differs significantly from the other UVA articles reviewed, and the experimental irradiation procedure and results are not clearly defined. Based on the articles selected, the threshold for UVA-induced apoptosis is between 3 and 6 hours, depending on dose.

Common assays to detect UVA-induced apoptosis are annexin V (FITC/PI) quantified with flow cytometry. This assay is an early marker of apoptosis as it detects the translocation of phosphatidylserine to the outer leaflet of the cell membrane (Breuckmann, von Kobyletzki et al., 2003). Fluorescent microscopy permits observation of nuclear fragmentation and membrane blebbing. Caspase-3 activity, mitochondrial transmembrane potential, and cytochrome c release from mitochondria are other methods employed for detecting later apoptotic events. The adherent cell-lines investigated in UVA-induced apoptosis studies include human mast cell line 1 (HMC-1), human squamous cell carcinoma-derived cell line (SCL- A431), and human epithelial carcinoma (HeLa) cells (Schindl, Klosner et al., 1998; Yao and Wang 2002; Guhl, Hartmann et al., 2003). Jurkat and H9 T lymphocytes are used in non-adherent cellular studies. The mechanisms involved in UV-induced apoptosis are complex, depending on factors such as cell line and UV wavelength.

Overview of UVB-Induced Apoptosis Studies

UVB-induced apoptosis results from both nuclear UV-mediated DNA damage (which triggers apoptosis via caspase-3) and cellular membrane effects (which activate caspase-8

leading to activation of caspase-3) (Kulms, Poppelmann et al., 1999). In this literature review comprised of 10 different works, the UVB doses range from 0.005 to 1 J/cm^2, which is considerably less than the UVA doses due to the higher photoxicity of a UVB photon. UVB post-exposure times range from 3 to 72 hours. Based on the UVB articles selected, the threshold for UVB-induced apoptosis occurs at 6 hours (0.025 J/cm^2) for HMC-1 cells, 12 hours (0.1 J/cm^2) for HeLa cells, 8 hours (0.25 J/cm^2) for HaCaT cells, 12 hours (0.256 J/cm^2) for human squamous cell carcinoma cells, and 24 hours (0.05 J/cm^2) for T lymphocytes. Based on the articles used in this review, the average threshold for UVB-induced apoptosis of 12.4 hours is longer than the average UVA-induced apoptosis threshold of 4.75 hours. UVB irradiation (0.5 J/cm^2) resulted in very few keratinocytes (HaCaT) cells remaining attached to the surface of the cell culture dish (Henseleit, Rosenbach et al., 1996).

Techniques used to detect UVB-induced apoptosis are annexin V (FITC/PI) and mitochondrial transmembrane depolarization by flow cytometry and cell death detection ELISA. Caspase-3 activity, release of cytochrome c, Poly (ADP-ribose) polymerase (PARP), a nuclear protein active in DNA repair in damaged cells, are also used in assays to identify apoptosis. Fluorescence, transmission electron, and confocal laser scanning microscopy techniques are used for morphological examination. Studies have successfully induced UVB-apoptosis in HeLa cells (Table 1.2).

UVA Dose and Mode of Exposure Compared to Prior Works

Additional biological effects of photoactivating light will be quantified using annexin V binding apoptosis assays to look at various UVA doses. Here we used two common photoactivation sources (intensities of 39.75 mW/cm^2 and 9 mW/cm^2) to apply relevant UVA photoactivating doses to HeLa cultures ranging from 0-24 J/cm^2 to explore apoptosis 18 hours after treatment. The 18-hr time point was optimized to be relevant for gene expression studies.

A UVB control (irradiance of 5.19 mW/cm^2 and dose of 0.93 J/cm^2) was included for comparison with the staurosporine chemically-induced apoptotic control. Cells were viewed by phase-contrast microscopy, and an annexin V-Cy5, and Propidium Iodide (PI) assay using flow cytometry was used to quantify live, dead, and apoptotic cells. Details of the assays are described further in the materials and methods found in chapter 2. Experiments were conducted with cells at room temperature and held at 4°C during photoexposure to explore thermal effects associated with photoactivation.

Thermal Effects Associated with UVA Photoactivation

Previous studies have found that exposing HeLa at temperatures below the transition temperature of the membrane (4ºC - 10ºC) prevents receptor clustering and is associated with reduced apoptosis (Rosette and Karin 1996). A temperature control plate system was designed to satisfy the low temperature requirement (4-10ºC) during UV light exposure and also explore the potential heating during photoactivation in this study.

Previous photoactivation studies using the B100-AP lamp have reported placing the sample on ice throughout the UV light exposure (Broitman, Amosova et al., 2003; Griffiths and Tawfik 2003). Therefore, temperature control instrumentation was constructed to study why cells exposed to high doses (> 5 J/cm^2) of 365nm light have decreased GFP expression as described earlier (Monroe, McQuain et al., 1999). The thermally-controlled plate used to monitor the sample temperature during photoexposure consists of a peltier-driven cold plate with a thermocouple and microprocessor for data acquisition as described in Chapter 2. The temperature increase describes the bulk media temperature since measurement of temperature at the site of cellular thermal injury is not possible with this system. Localized thermal gradients introduced by light exposure could influence cellular effects; therefore, light exposure studies

Table 1.1 UVA-Induced Apoptosis Review

Source	Irradiance (W/cm^2)	Dose (J/cm^2)	Cell line	Exposure Time	Post-Eposure (hr)	Apoptosis threshold	Assays	Manuscript
*UVA1 (340-400 nm), RT	0.0069	5, 10, 15, 20, 25	HMC-1 (human mast cell line1)	12 min-1 hr	3, 6, 12, 24, 48, 72	6 hr (10 J/cm^2)	Vybrant kit #4 (YO-PRO-1/PI) by flow cytometry; Caspase-3; Nuclear extracts; Mitochondrial transmembrane depolarization; Cytochrome c	(Guhl, Hartmann et al., 2003)
UVA1 (340-400 nm) Photomed CL (Germany), RT	0.025	2.5, 5, 10, 15, 20, 30, 40, 60	T lymphocytes	1.6 min-40 min	3, 6, 24, 48	6 hr (10 J/cm^2)	Annexin V (FITC/PI) by flow cytometry; Fluorescence microscopy (AO/EB)	(Breuckmann, von Kobyletzki et al., 2003)
UVA1 (365 nm) UVASUN sunlamp (Germany) d=31 cm, RT	0.02	20, 40, 60, 80	Jurkat, H9 T lymphocytes	16-67 min	4, 24	4 hr (20 J/cm^2)	Transmission electron microscopy; Annexin V & Mitochondrial transmembrane potential by flow cytometry	(Godar 1999)
UVA1(340-390nm) & UVA (315-390nm) Metal halide lamp filtered (Mutzhas Supersun 5000, Germany), d= 30 cm, 25°C	*	8, 16, 32, 48, 64, 80, 96	human squamous cell carcinoma-derived cell line A 431	*	3, 6, 12, 24, 48	3 hr (96 J/cm^2)	Annexin V (FITC/PI) by flow cytometry	(Schindl, Klosner et al., 1998)
*UVA	5.07E-07	0.00365	HeLa	2 hr	2	+	Annexin V by flow cytometry	(Yao and Wang 2002)

* indicates information not given in the paper

\+ confirms apoptosis was induced, though time not stated

Table 1.2 UVB-Induced Apoptosis Review

Source	Irradiance (W/cm^2)	Dose (J/cm^2)	Cell line	Exposure Time	Post-Exposure (hr)	Apoptosis Threshold	Assays	Manuscript
(280-315 nm) Waldmann UV800 light source (Germany), RT	0.00083	0.005, 0.025, 0.05, 0.075, 0.1	HMC-1	6 s – 2 min	3, 6, 12, 24, 48, 72 hr	6 hr ($0.025J/cm^2$)	Vybrant kit #4 (YO-PRO-1/PI) by flow cytometry; Caspase-3; Transmission electron microscopy; Mitochondrial transmembrane depolarization; Cytochrome c	(Guhl, Hartmann et al., 2003)
(280-320 nm) UV-Multiester (Germany), RT	*	0.01, 0.05, 0.10, 0.30, 0.50, 1.0	T lymphocytes	*	3, 6, 24, 48 hr	24 hr ($0.05\ J/cm^2$)	Annexin V (FITC/PI) by flow cytometry; Fluorescence microscopy (AO/EB)	(Breuckmann, von Kobyletzki et al., 2003)
(313 nm) bank of six TL12 fluorescent bulbs (Philips), RT	*	0.04	HeLa	*	16 hr	+	Cell detection ELISA, Cytochrome c; Confocal laser scanning microscopy (CD95 activation)	(Kulms, Dussmann et al., 2002)
(313 nm) bank of six TL12 fluorescent bulbs (Philips), 4^oC & 37^oC	0.001	0.04	HeLa	40 s	16 hr	+	Cell detection ELISA; Cytochrome c (IL-6)	(Kulms, Poppelmann et al., 2000)
(313 nm) FS20 bulbs (Westinghouse), 4^oC & 37^oC	*	0.04	HeLa	*	16 hr	+	Cell detection ELISA; Caspase-3; PARP; Southwestern dot-blot (nuclear & membrane)	(Kulms, Poppelmann et al., 1999)

(Table 1.2 continued)

48% (280-320 nm), 52% UVA 2 Airam LUB UV fluorescent tubes, dist. = 20 cm, RT	0.0011	0.1	HeLa	*	8, 12, 24 hr	12 hr (0.1 J/cm^2)	PI staining (apoptotic nuclei in sub-G_o population) by flow cytometry; Light microscopy; Fluorescence microscopy (nuclear fragmentation and membrane blebbing)	(Isoherranen, Sauroja et al., 1999)
(313 nm) FS20 bulbs (4), 10^{o}C (30 min. prior and exposure)	*	0.03	HaCaT	*	0.5, 2, 4, 8, 16 hr	+	Cell detection ELISA; FITC- labeled Annexin V with flow cytometry; PARP; Confocal laser scanning microscopy	(Aragane, Kulms et al., 1998)
(290-320 nm) Metal halide lamp filtered (Mutzhas Supersun 5000, Germany) d= 30 cm, 25^{o}C	*	0.008, 0.032, 0.048, 0.064, 0.096, 0.128, 0.192, 0.256	human squamous cell carcinoma-derived cell line A 431	*	3, 6, 12, 24, 48 hr	12 hr (0.256J/cm^2)	Annexin V (FITC/PI) by flow cytometry	(Schindl, Klosner et al., 1998)
(307-312 nm) *source not given, 10^{o}C incubation	*	0.06	HeLa	5, 15, 45 min	fixed at exposure time intervals	○	Confocal microscope; Immunoblotting assays (kinase activity)	(Rosette and Karin 1996)
(313 nm) Philips TL 20W/12 light source, RT	*	0-0.5	HaCaT	*	2, 6, 8, 24, 48 hr	8 hr (0.25 J/cm^2)	Light and electron microscope; Cell detection ELISA	(Henseleit, Rosenbach et al., 1996)

* indicates information not given in the paper
\+ confirms apoptosis was induced, though time not stated
○ apoptosis assays not performed, significant to thermal effects studies

were conducted with samples held at various temperatures to separate thermal from other forms of light-induced injury.

Research Significance and Project Objectives

The overall goal of this project is to describe the molecular events at the cell level that result in decreased GFP expression at high UVA light exposure levels. The specific aim of this project is to determine biological effects of 365nm light on HeLa cells in order to establish acceptable doses of UVA that can be applied to HeLa cells for photoactivation applications. While light at 365 nm is thought to have minimal biological effects, further research is needed to verify this assumption for the light exposures required for photoactivation. The UVA threshold for cells determined in this study provides important photobiological information applicable to all photoactivation studies requiring UVA light, including caging techniques and recent fluorescence techniques for studying molecular interactions in live cells. This was accomplished in several steps. First, the UV light sources were characterized so that the desired wavelengths of light could be selected, and a detailed understanding of the spectral output and irradiance of each light source were known. Next, to determine if localized heating or UVA contributes to cell response, experiments were conducted at different temperatures to evaluate the sample heating due to the light source. Finally, the dose-response of UVA was used to determine the threshold of UVA that cells can withstand during photoactivation. Various doses and durations of UV light were used to assess light-tissue thermal interactions and apoptotic effects of the light sources.

Chapter 2

Quantitative Effects of 365nm Photoactivating Light on HeLa Cells

Introduction

UVA light (320-400nm) is commonly used in molecular methods of photoactivation. Photoactivation is the light-induced activation of an inert molecule to an active state, such as converting the molecule of interest into a fluorescent state so the molecule can be tracked in living cells. The ability to temporally and spatially control photoactivatable proteins has resulted in their wide use to study protein behavior in living cells. Photoactivation is also commonly used in the ultraviolet-light-induced release of a caged group from a "caged" compound. Caged compounds have a covalently attached group that renders the target molecule inert and is released upon light exposure in order to restore activity of the target molecule; one example includes caged ATP that has a single cage that blocks bioactivity (Kaplan, Forbush et al., 1978). Caged chemistries are now being used to control activities of larger biomolecules, such as proteins and nucleic acids, which require more attached cages per target molecule, therefore necessitating increased light doses to achieve more total recovery of activity. The use of light for studies at the molecular level highlights the need for understanding the cellular response to UV-induced stress, including cytotoxic-apoptotic effects, DNA damage, and activation of various cellular stress genes (Meunier, Sarasin et al., 2002). In contrast to classic photolysis experiments which study fast kinetic responses in a matter of seconds (e.g. ATP), relatively longer-term studies, such as the study of gene expression and metabolic pathways, require resumption of cell health several days after photoexposure. Biological effects, including apoptosis, photomutagenesis, chromosomal damage, and cellular response to UV-induced DNA lesions, are sufficient to evaluate photobiological cell pathology (Meunier, Sarasin et al., 2002).

Ultraviolet radiation consists of three ranges: UVA (320-400 nm), UVB (290-320 nm), and UVC (200-290 nm). Short UV radiation effects on DNA are well known. UVC and UVB are known to induce the p53 pathway, whereas the role of UVA depends very specifically on cell type and is not as clear (Meunier, Sarasin et al., 2002). The toxicity of a UVA photon is described as "one thousand times smaller than that of a UVC photon and about one hundred times smaller than that of a UVB photon" (Giacomoni 1995). Ultraviolet radiation affects various cell targets including DNA, cell surface receptors, kinases, phosphatases, and transcription factors (Kulms and Schwarz 2002). The biological effects including mediator release, altered surface receptors, and apoptosis induction of UV radiation occur when a cellular chromophore absorbs UV radiation and transduces the energy into a biochemical signal (Kulms, Poppelmann et al., 2000). UVA (320-400 nm) light is commonly used for photoactivation of the caged molecules described earlier. While UVA doesn't possess the high energy of UVC light, it has been shown to cause a cellular response in HeLa cells at high doses (Monroe, McQuain et al., 1999). A decrease in GFP expression was noted at increasing doses of UVA light exposures. Little is known about the exact molecular mechanisms involved in UVA-induced apoptosis (He, Huang et al., 2004). It has been proposed that the initiation of biological effects of UVA radiation involves the absorption by a non-DNA chromophore, which causes the generation of oxygen species or upregulation of critical target molecules (Tyrrell and Keyse 1990).

Apoptosis is a programmed cell death where the cell undergoes very specific biochemical and morphological events. The apoptotic cascade of events includes condensing chromatin, cell shrinkage and blebbing, loss of asymmetry of the plasma membrane, and formation of apoptotic bodies, which are eventually engulfed by phagocytosis without causing inflammation (Kerr, Wyllie et al., 1972). Inappropriate regulation of apoptosis results in disease. For therapeutic

intervention, a clear understanding and ability to detect and control apoptotic events are important.

Temperature conditions have been found to play a role in cellular apoptotic effects that occur during photoexposure studies. Previous studies have found that exposing HeLa cells at temperatures below the transition temperature of the membrane (4ºC - 10ºC) prevents receptor clustering and is associated with reduced apoptosis caused by UVB (Rosette and Karin 1996). A mercury-arc photolysis system has been used for caged IP_3 (inositol triphosphate) and caged cAMP studies. The system consisted of a housing for heat dissipation and a water-jacketed IR filter to prevent heating of the sample chamber during the 10-minute exposure of endothelial cells (Patton, Alexander et al., 1991). Previous studies have employed the use of the BlakRay B100 AP (UVP) lamp for irradiation of cells placed on ice during photoactivation (Broitman, Amosova et al., 2003; Griffiths and Tawfik 2003). To investigate the effects of temperature-controlled photoexposure, a temperature control and measurement system was designed for this study.

Although light at 365 nm is thought to have minimal biological effects, the goal of this was to determine the UVA dose threshold for HeLa cells used in photoactivation studies. Here we use two well-characterized light sources to assess the effects of 365nm light on cell viability using qualitative morphological assessment and a quantitative approach employing flow cytometric analysis of an annexin V apoptosis assay. These thresholds are important for designing photoactivation studies to achieve optimal light activation without damaging the cells.

Materials and Methods

Methods Overview

In brief, several techniques were employed to describe the photobiological and thermal effects of UVA light on cell cultures. Light sources used for photoactivation were characterized

in terms of their spectral output and irradiance. A temperature measurement and control system was designed for this study to assess the increase in temperature associated with photoexposure and also explore if cooling could prevent photothermal effects on cells. Phase-contrast microscopy was used to visualize morphological changes after photoexposure. More quantitative responses were analyzed with an apoptosis flow cytometry assay.

Materials

All reagents for cell culture were purchased from HyClone Laboratories, Inc. (Logan, UT), unless otherwise stated. Annexin V-Cy5 was purchased from MBL International Corporation (Woburn, MA). Staurosporine and Propidium Iodide were purchased from CalBiochem (EMD BioSciences, Darmstadt, Germany).

Cell Culture

HeLa cells (human epithelial carcinoma cells) (American Type Culture Collection) were maintained in 25-cm^2 flasks (BD Falcon, Franklin Lakes, NJ) with 5ml of Dulbecco's Modified Eagle's Medium-reduced serum (DMEM-RS) supplemented with 3% Fetal Bovine Serum (FBS) and incubated at 37ºC and 5% CO_2. HeLa cells were plated at a density of 80,000 cells/cm^2 in 35-mm optically clear polystyrene cell culture dishes (Corning, Corning, NY). Cells were allowed to adhere and grow for 24 hours prior to photoexposure.

UVA Light Source Characterization

The mercury B100-AP lamp (UVP Inc., Upland, CA) has a narrow peak output at 365nm and an irradiance of 10.33 mW/cm^2 at 15 cm and 9.00 mW/cm^2 with the IR filter (818-ST-UV detector, Newport Corporation, Irvine, CA). Spectrographic characterization of this lamp confirmed that the emission spectrum is 365±8 nm (USB2000 Fiber Optic Spectrometer, Ocean Optics, Inc., Dunedin, FL). A heat-absorbing filter (Schott KG-2; Germany; 50.8mm square, 2mm thick) was used with the B-100-AP lamp to attenuate infrared heat with the UVP B-100-AP

lamp. The filter has a transmittance of greater than 85 percent at 365nm and less than 10 percent at 1100nm to absorb unwanted heat from the light source. The heat-absorbing filter was used to prevent any cellular damage resulting from heat dissipation by the light source.

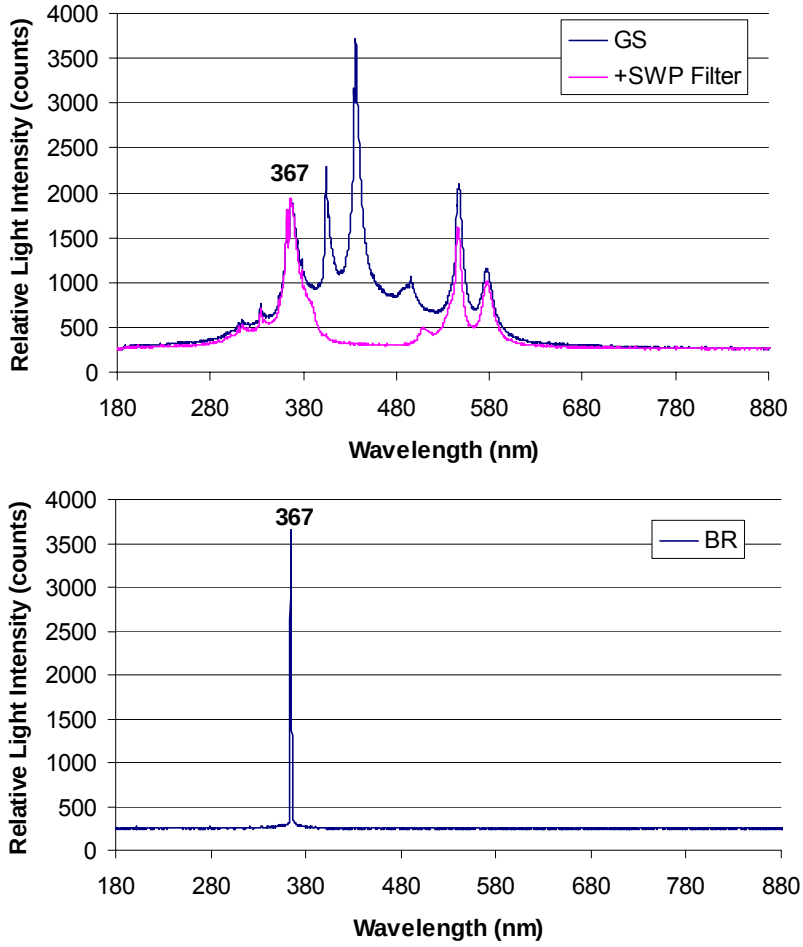

Figure 2.1 Light source spectral characterization

A higher intensity GreenSpot 100-watt super pressure mercury lamp with a 5mm x 1000mm light guide (American Ultraviolet, Lebanon, IN) was combined with a short bandpass filter to block wavelengths above the desired test wavelength. The GreenSpot photocuring system is commonly used in the semiconductor industry. The GreenSpot lamp supplies an irradiance at 4.2 cm of 112.25 mW/cm^2 and 39.75 mW/cm^2 with the short bandpass and IR filters (818-ST-UV detector, Newport Corporation, Irvine, CA). Approximately 60% of the filtered GreenSpot spectra falls in the 365±8nm bandwidth. Intensity measurements were taken with each filter to ensure the energy output was correct. The short wavelength pass filter (SWP-2502U-400; Lambda Research Optics, CA; diameter 25.4mm; 1.5mm thick) has a sharp cut off at 400nm and transmittance greater than 90 percent at 365nm to select for common UVA photoactivating

wavelengths. Spectra of the BlakRay and GreenSpot with and without the filter are shown in Figure 2.1.

Photoexposure Protocol

The B100-AP, GreenSpot, and Transilluminator lamps described were used for all UV light experiments. The light sources were allowed to warm-up for ten minutes before each cell experiment. The DMEM-RS was aspirated, and 1.5mL of phenol-free OptiMEM reduced protein medium (Invitrogen Corporation, Grand Island, NY) was added to the cells. The cells in the dish were consistently placed under the center of the lamp with the lid on, providing a uniform intensity across the dish. After the cells were exposed to a specific light dose, the Opti-MEM was replaced with 1.25mL of fresh DMEM-RS and FBS. The cells were allowed a recovery period of approximately 18 hours in a 37ºC incubator with 5% CO_2. After this period of time, the cells were imaged using phase-contrast light microscopy and then assessed with an apoptosis photodamage assay on the BD FACSAria flow cytometer (BD Biosciences). Each experimental cell treatment was performed in triplicate.

Temperature Control System

To determine if the light sources used generate heat, a thermally controlled plate was constructed to measure and control sample temperature during photoexposure. The system consisted of a peltier-driven cold plate with a thermocouple and microprocessor for data acquisition (Fig. 2.2).

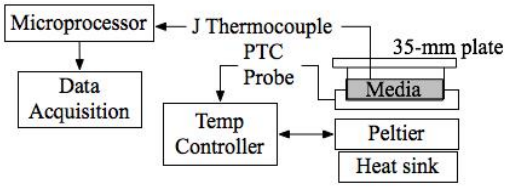

Figure 2.2 Control and measurement system for light-induced thermal effects on cell cultures.

The thermocouple was placed through a 0.6 cm-diameter hole in the lid and shielded with aluminum foil to prevent direct UV absorption by the thermocouple. The thermoelectric cold plate (TCP-30, Advanced Thermoelectric, Nashua, New Hampshire) had a four-inch square surface and functioned using peltier element principles. The TCP-30 operated from -15ºC to 75ºC and has control accuracy of ±0.1ºC. A fan and heat sink, located below the peltier element, was used to remove the excess heat on the hot side of the peltier element (Fig. 2.3). The top aluminum surface located above the peltier element was controlled according to the set point temperature of the temperature controller. The TDH01 Temperature Controller (Tecnologic, Vigevano, Italy) was a digital microprocessor-based controller with a single set point and ON/OFF control mode. The unit had one input for the positive temperature coefficient (PTC) probe, which was used to measure the cold plate temperature. The PTC probe measurement range is -9.9ºC to +99.9ºC with a sampling rate of one sample/second and overall accuracy of ±0.55 ºC. The temperature controller parameters (decimal point, unit of measurement, output operating mode, input probe) were programmed using the front panel. The temperature of the solution was measured using a type J (Iron/Constanstan) thermocouple with the DS2760 thermocouple kit (#28022) (Parallax, Rocklin, CA). The thermocouple module and basic stamp 2p were used with the basic stamp 2p24 demo board for data acquisition. Serial PC interface was used to program the basic stamp and collect data (Appendix B). A laptop with a serial port was used for running the StampDAQ™ Basic Stamp® Data Acquisition program.

Figure 2.3 The BlakRay light source and peltier-driven cold plate with temperature controller are shown.

Temperature Effects Protocol

A 35mm cell culture dish of Opti-MEM was taken from room temperature and placed under the UV BlakRay lamp and GreenSpot as described previously. The cell culture dish temperature was recorded using a basic stamp 2p thermocouple kit and laptop computer for data acquisition at 1Hz, with one thermocouple per dish for three separate photoexposures and a moving average of 10 points was used for smoothing. The cold plate was allowed to reach steady-state before the cell culture media dish experiment was conducted for cooling treatments.

UVB Irradiation

A high performance Transilluminator (TFM-20, UVP Inc., Upland, CA) was used as a UV-B-light-induced apoptotic control. The Transilluminator supplies an irradiance of 5.19 mW/cm^2 with a narrow peak output at 302nm (818-ST-UV detector, Newport Corporation, Irvine, CA). The cell culture dish was irradiated from below for the UVB control.

Brightfield Phase-Contrast Microscopy

Images were acquired with an inverted Eclipse TS100 Nikon fluorescence microscope using 10X and 40X objective lenses and a CoolSnapFX camera (Photometrics, Tucson, AZ). Image processing was performed on a Windows computer using MetaVue software (Universal Imaging Corporation, West Chester, PA). Following UVA irradiation and the 18-hr recovery period, HeLa cells were imaged by brightfield phase-contrast microscopy at 10X and 40X magnification.

Annexin V-Cy5/PI Apoptosis Assay and Analysis

For chemical apoptosis induction, cells were incubated in fresh medium enriched with 0.25 μM staurosporine (CalBiochem, EMD BioSciences, Darmstadt, Germany), a protein kinase inhibitor known to induce apoptosis, at various time points to determine when the apoptotic morphological changes occurred (Appendix D). For a late apoptotic/necrotic control, cells were

incubated in fresh medium enriched with 2mM hydrogen peroxide for 18 hours. The negative control consisted of cells treated with fresh medium, free from inducing agents (staurosporine, hydrogen peroxide, or UV light).

For each treatment, detached and attached cells were pooled, harvested by trypsinization (0.25% trypsin), washed with 200µl of culture medium, and resuspended in 200µl of 1X Media Binding Buffer (MBL International Corporation, Woburn, MA) (Appendix A). The use of the annexin V/PI method is similar to the methods published by Koopman, Reutelingsperger et al., (1994). 200 µl of cell suspension was mixed with 4µl of annexin-V-Cy5 and 6µl of 30µg/ml Propidium Iodide (Annexin V Biotin Apoptosis Detection kit, Oncogene Sciences, San Diego, CA) in a flow cytometry tube and incubated in the dark at room temperature for 20 min. Liquid volume was removed by centrifugation and aspiration, and the cells were resuspended by gentle vortexing in 200 µl of PBS with calcium and magnesium to be analyzed on the flow cytometer. Approximately 20,000 cell events were collected on the BD FACSAria flow cytometer equipped with 488nm and 633nm lasers. Fluorescence and scatter dotplots were acquired in list mode and analyzed using WinMDI 2.8 software (by Dr. J. Trotter, Scripps Institute, La Jolla, CA).

Statistical Analysis

All values are indicated as mean ± SEM. Student's t-test was employed, with $p \leq 0.05$ considered to be significant. Each "n" replicate was composed of a single dish and treatment in which 20,000 cell events were analyzed, and each experiment was conducted in triplicate.

Results

Thermal Effects of Light Exposure

Temperature measurements indicate that the cell culture dish media experienced a 5.2ºC temperature increase during a continuous 20-minute BlakRay light exposure at room temperature, while the controlled cold plate (4ºC) had a reduced temperature change of -0.9ºC

(Fig. 2.4). Use of the heat absorbing infrared filter with the BlakRay resulted in a 3ºC increase during exposure. The GreenSpot light source produced less heating, resulting in a 1.4ºC temperature increase at room temperature and a -1.1ºC temperature change when exposed with the cold plate maintained at 4°C. Localized temperature increases introduced by light exposure could explain some of the cellular effects seen in prior photoactivation studies, providing justification for future studies with 365nm light exposure where samples were held at room temperature and 4°C to separate thermal from other forms of light-induced injury.

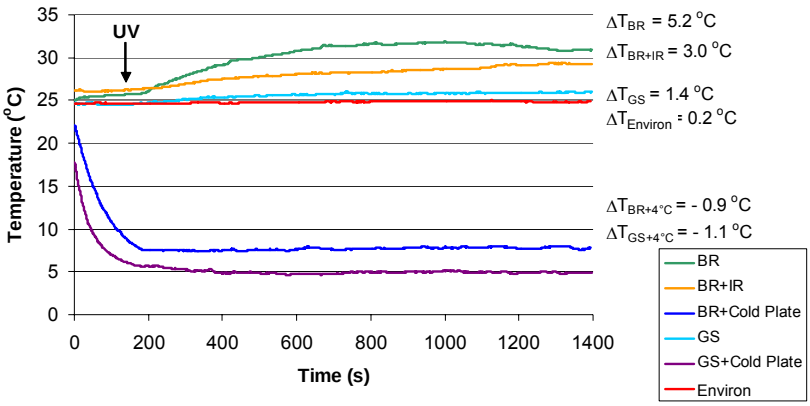

Figure 2.4 Temperature increase due to UVA light sources.

UVA Cell Damage Assessed by Microscopy of Adherent Cells

Following UVA irradiation and the 18 hr recovery period, HeLa cells were imaged by brightfield phase-contrast microscopy. Negative control cells not receiving UV or chemical treatment were imaged at 10X and 40X magnification. The live HeLa control cells have normal morphology as illustrated in Fig. 2.5 (a). The majority of hydrogen-peroxide-treated late apoptotic/necrotic control cells became detached with the few remaining showing signs of damaged cell membranes and organelles (Fig. 2.5 (b)). The morphological changes of the UVA-treated cells are not as severe, but do include large membrane blebbing and cell shrinkage (Fig. 2.5(c)).

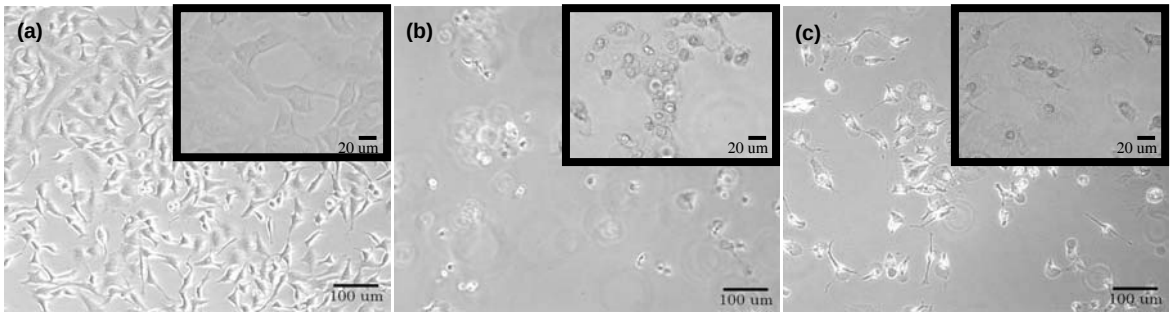

Figure 2.5 Phase-contrast images (40X and 10X) of (a) Live, (b) Dead, and (c) UVA-treated (10.74 J/cm^2) HeLa cells (10X images scale bar = 100 μm). Inset images are of the same samples at 40X (40X scale bar = 20μm).

UVA Cell Damage Assessed by Flow Cytometry

The scatterplot illustrates information on the condition of the cells from the shape/distribution and provides the basis for analyzing the fluorescence dotplots. All fluorescent dotplots were gated on a region (R1) that was created in the scatterplot for the live control as shown in Figure 2.6 (A). This was done to account for a more homogeneous cell population and eliminate cellular debris so that the various treatments could be compared. The necrotic (dead) control scatter (Fig. 2.6 (B)) shows a decrease in cell size and more internal granularity compared to the live (Fig. 2.6 (A)). The UV-treated plots (Fig. 2.6 (D)-(F)) show increasing amounts of cell debris.

Apoptosis is characterized by phosphatidylserine (PS) translocation from the inner leaflet to the outer leaflet of the lipid bilayer, while the cell membrane remains intact. Annexin V has a high affinity for PS in the presence of calcium, and PS translocation is detected by Cy5 fluorescence from the conjugated annexin V-Cy5 complex. Propidium iodide (PI) staining of the cells indicates that the integrity of the cell membrane has been compromised and is used to distinguish living and early apoptotic cells from late apoptotic/necrotic cells. Dead cells will have high PI and Cy5 fluorescence, and apoptotic cells will show high Cy5 fluorescence with low PI. Live cells will have low PI and Cy5 fluorescence.

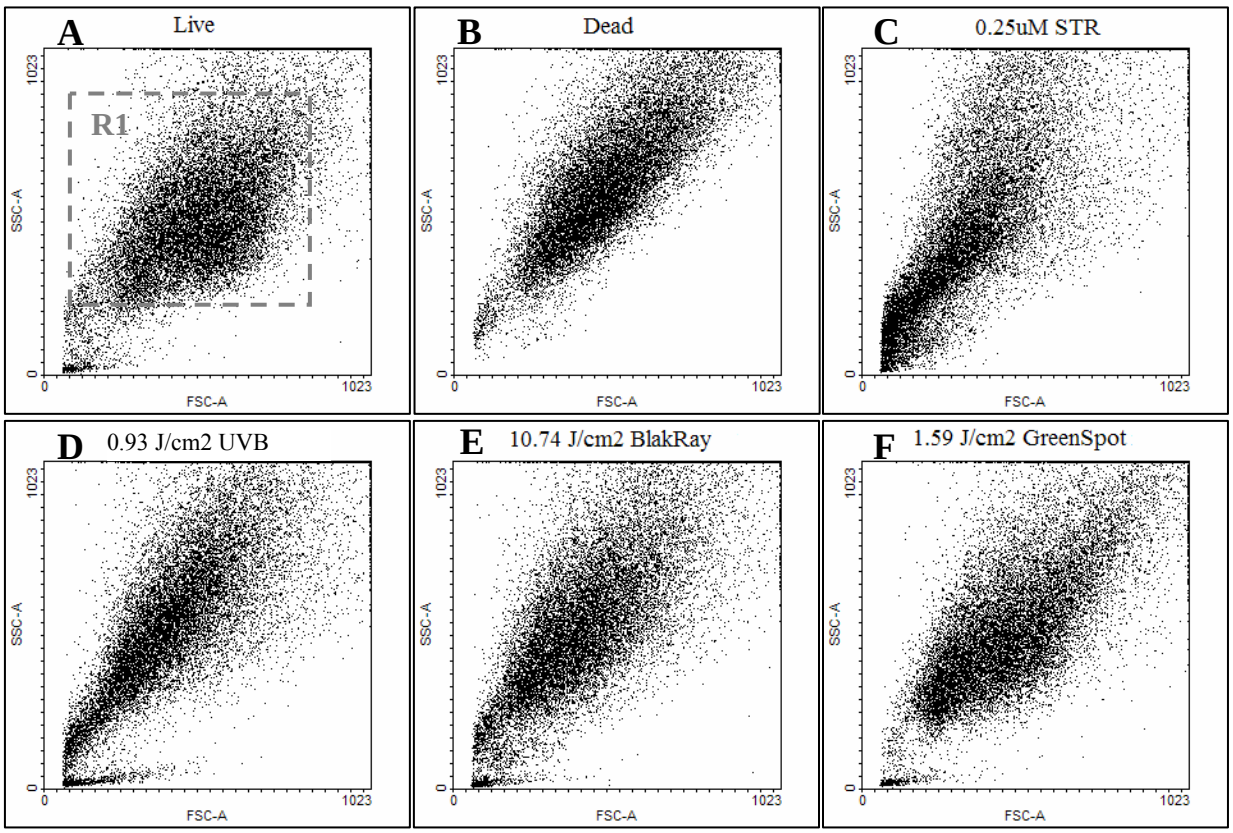

Figure 2.6 (A-F) Qualitative cytometer scatterplot comparison among treatments, (A) Live, (B) Necrotic, (C) 0.25μM Staurosporine (STR), (D) 0.93 J/cm^2 UVB, (E) 10.74 J/cm^2 BlakRay, (F) 1.59 J/cm^2 GreenSpot. Region1 (R1) shown in (A) was used to determine the cell population for fluorescence dotplot analysis.

Quadrant analysis was performed on the gated fluorescence dotplot to quantify the percentage of live, necrotic (dead), and apoptotic cell populations. UVA-induced cell death appears to follow a similar path to UVB-induced cell death, in terms of membrane integrity and PS translocation, which was detected by the annexin V assay and provides validation for the chemical-induced control (0.25 μM Str) by its similarity to the UVB light- induced control (Fig. 2.7 (C), (D)). These apoptotic controls ((C) (D)) exhibit an increase in Cy5 staining towards the lower right quadrant. The BlakRay treatment (E) shows an increase in necrotic cells in the upper right quadrant, thus indicating that the BR is lethal to cells at a dose of 10.74 J/cm^2. The GreenSpot treament of 1.59 J/cm^2 (F) appears far less damaging to cells, with the majority of

cells in the lower left (live) quadrant. The dotplots show a stray population of low annexin V-staining for the dead control similar to what has been noted in other works (vanEngeland, Ramaekers et al., 1996; Del Bino, Darzynkiewicz et al., 1999).

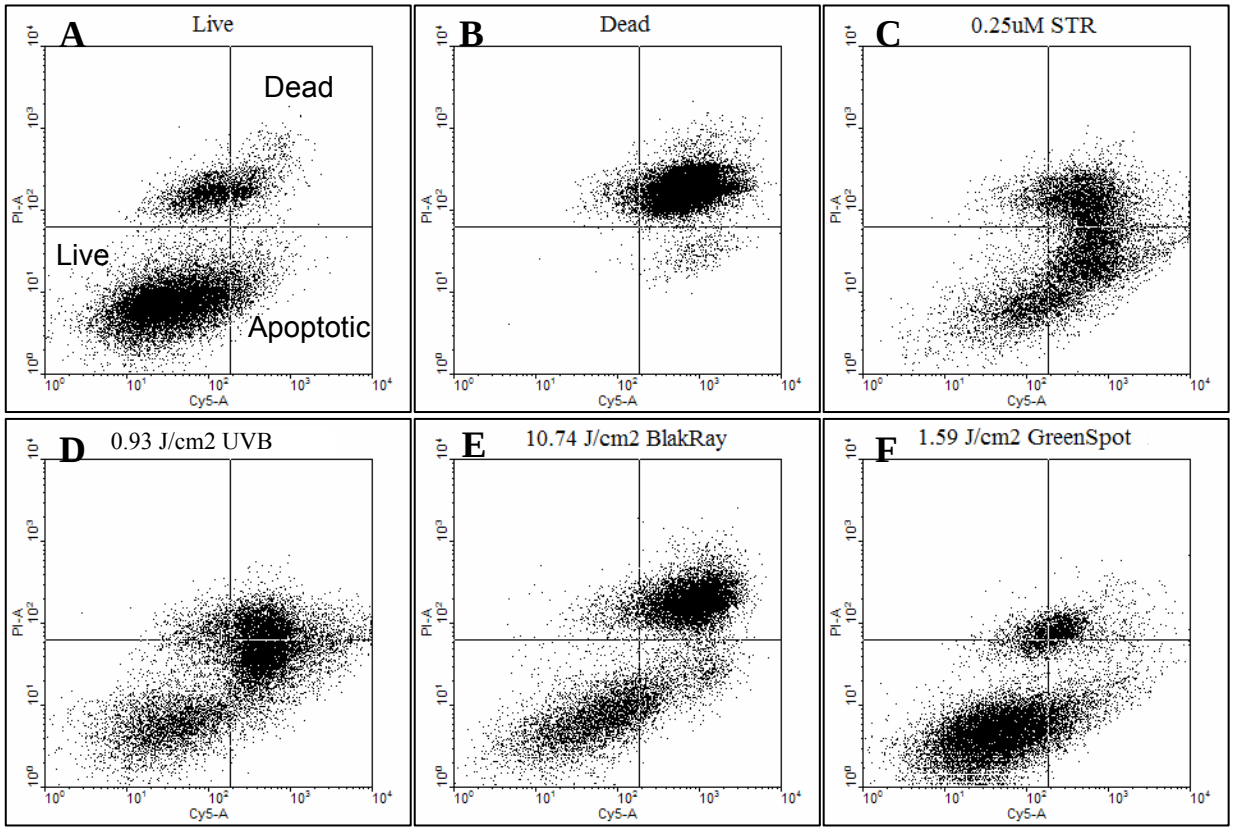

Figure 2.7 (A-F) Qualitative cytometer fluorescence dotplot comparison among treatments, (A) Live, (B) Necrotic, (C) 0.25μM Staurosporine (STR), (D) 0.93 J/cm^2 UVB, (E) 10.74 J/cm^2 BlakRay, (F) 1.59 J/cm^2 GreenSpot.

Importance of Cell Confluence for Cell Health

The importance of cell confluence for the live control was observed from the week-to-week experiments. Cell confluence was found to affect the cell's health, as well as sensitivity to UVA light as described later in this manuscript. The nominal density for cell experiments was 80, 000 cells/cm^2. A large variability in health was observed at lower cell density as shown in Fig. 2.8. Cells seeded at a lower cell density (8,000 cells/cm^2) had the highest percentage of

apoptotic and dead cells (34 ±6% and 25 ±3% respectively) and the lowest percentage of live cells (41±9%). The cells seeded at highest density (800,000 cells/cm^2) had a significant difference in dead cells with 7 ±0.01% compared to the 80,000 cells/cm^2-seeded cells 9 ±0.2%, though there was no significant difference in the percentage of apoptotic cells. Cells seeded at 80,000 cells/cm^2 had 84 ±1.6% live cells and were not significantly different from the 800,000 cells/cm^2-seeded cells, which had 88 ±0.3% live cells.

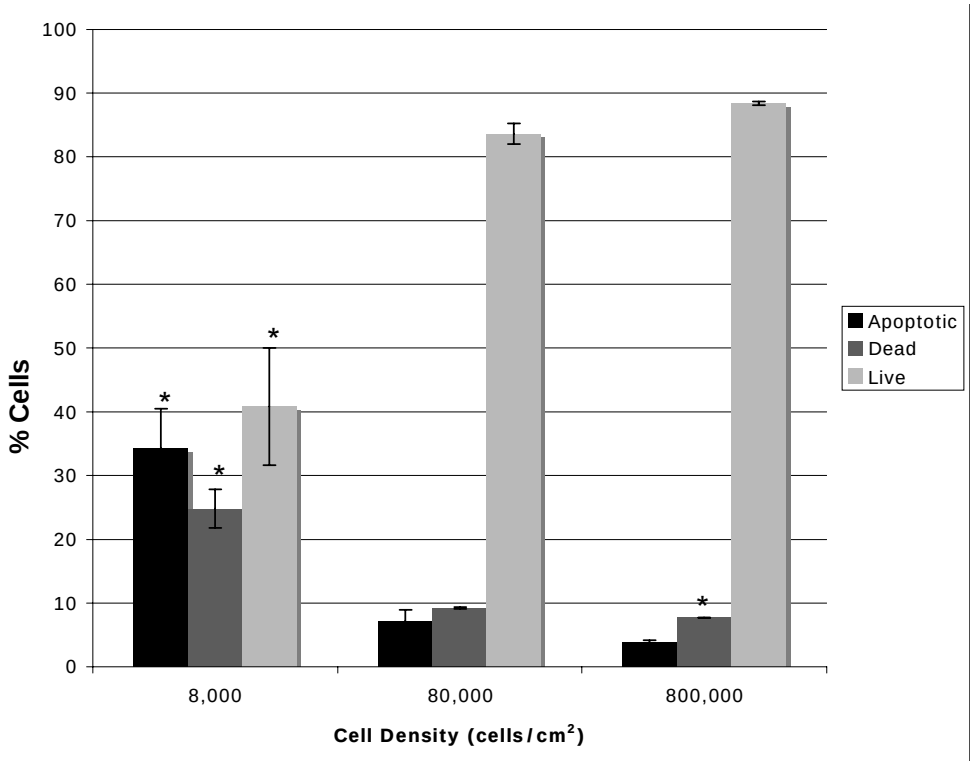

Figure 2.8 Effect of cell density on annexin V apoptosis assay protocol ($p \leq 0.05$, Student's t-test).

Cell seeding density was also found to affect cells' sensitivity to UVA light. Experiments employing the GreenSpot with different initial cell seeding densities (low (approximately 20,000 cells/cm^2) and high (approximately 100,000 cells/cm^2)) resulted in very different dose-response curves as seen in Fig. 2.9. While a dose of 4.8 J/cm^2 resulted in 51

±2.8% dead and apoptotic cells in low-seeded dishes, the higher density cells required 5 times the dose (23.85 J/cm^2) to produce approximately 48 ±3.2% dead and apoptotic cells.

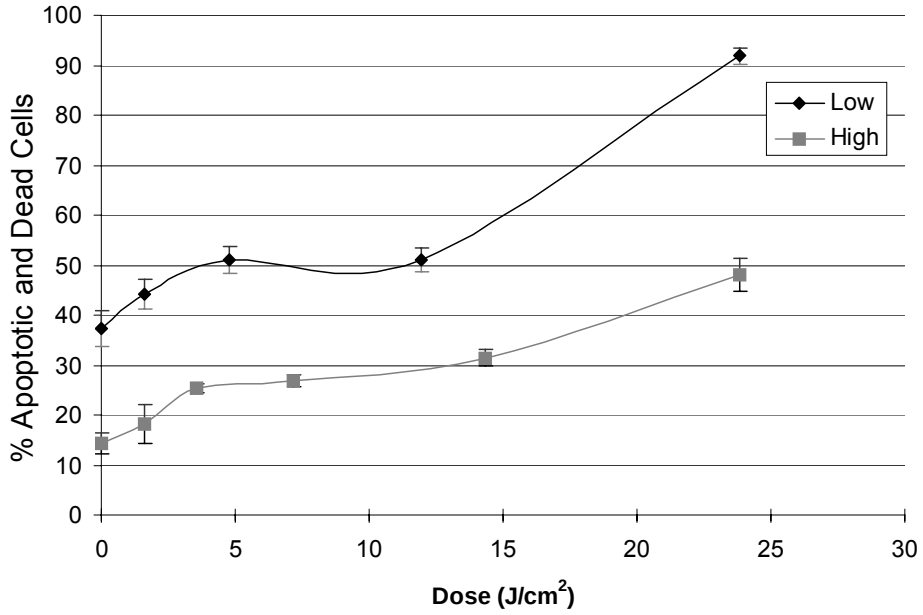

Figure 2.9 Dose-response for the GreenSpot with different cell seeding densities.

Dose-Response for the GreenSpot and BlakRay

Dose-response curves for the GreenSpot and BlakRay light sources were determined. Doses for each light source were applied with a maximal dose of 23.85 J/cm^{2}on the GreenSpot (Fig. 2.10). No significant GS damage was seen at 1.6 J/cm^2 ($p \leq 0.05$, Student's t-test). The GreenSpot (GS) shows significantly less photodamage than the BlakRay (BR). The maximum dose of 23.85 J/cm^2 on the GreenSpot resulted in 78 ±6% dead and apoptotic cells while the maximum dose of 11 J/cm^2 on the BlakRay resulted in 96 ±0.7% dead and apoptotic cells. The BlakRay was found to induce 50% dead and apoptotic cells with a dose of 2.7 J/cm^2 while the equivalent amount of damage by the GreenSpot requires a 7.2 J/cm^2 dose.

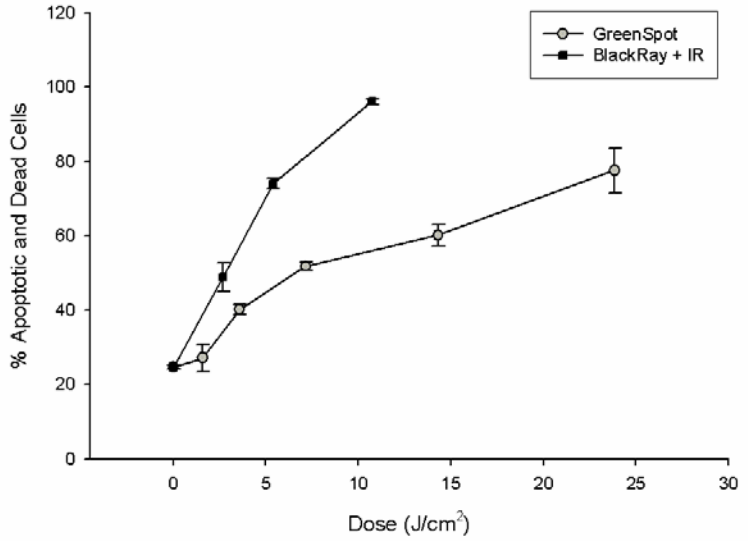

Figure 2.10 Dose-response of UVA light sources

Modeling Dose-Response of GS and BR

Dose-responses for the two light sources used were modeled with exponential rise to maximum functions. The dose of UVA in which 50% of the cells are found to be apoptotic and dead is referred to as the $dose_{1/2}$. Modeling the dose-response allows a $dose_{1/2}$ to be determined. Models were created in SigmaPlot 9, where:

y = % apoptotic and dead cells

x = UVA dose (J/cm^2)

Modeling GreenSpot Dose-response (Fig. 2.11)

$$y = 24.06 + (65.46)(1 - e^{-(0.066)(x)}) \quad (1)$$

$$R^2 = 0.9784$$

$$dose_{1/2\ GS} = 7.60\ J/cm^2$$

Modeling BlakRay Dose-response (Fig. 2.12)

$$y = 23.94 + (101.01)(1 - e^{-(0.1186)(x)}) \quad (2)$$

$$R^2 = 0.9952$$

$$dose_{1/2\ BR} = 2.52\ J/cm^2$$

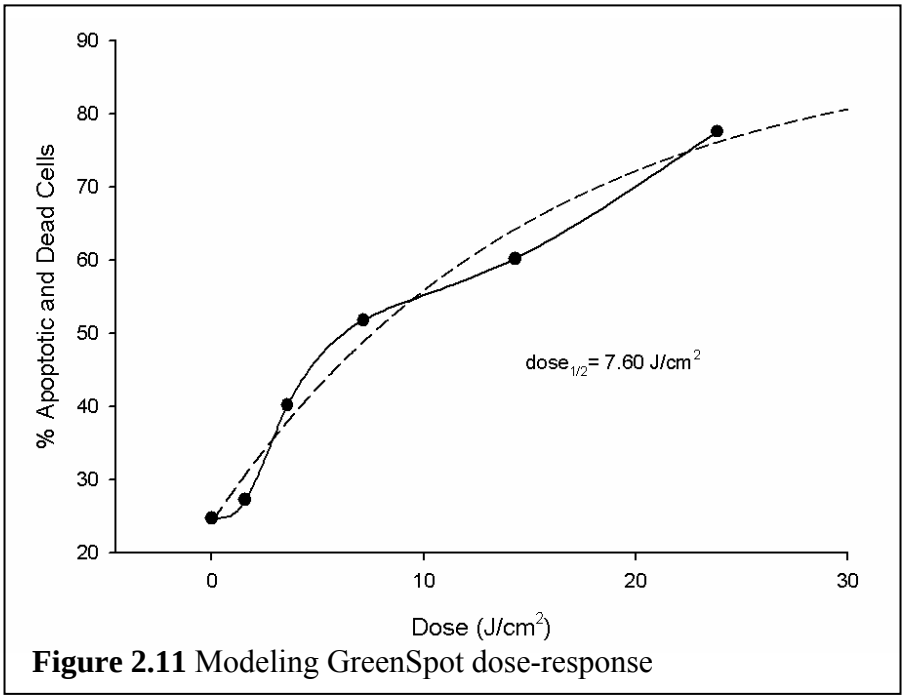

Figure 2.11 Modeling GreenSpot dose-response

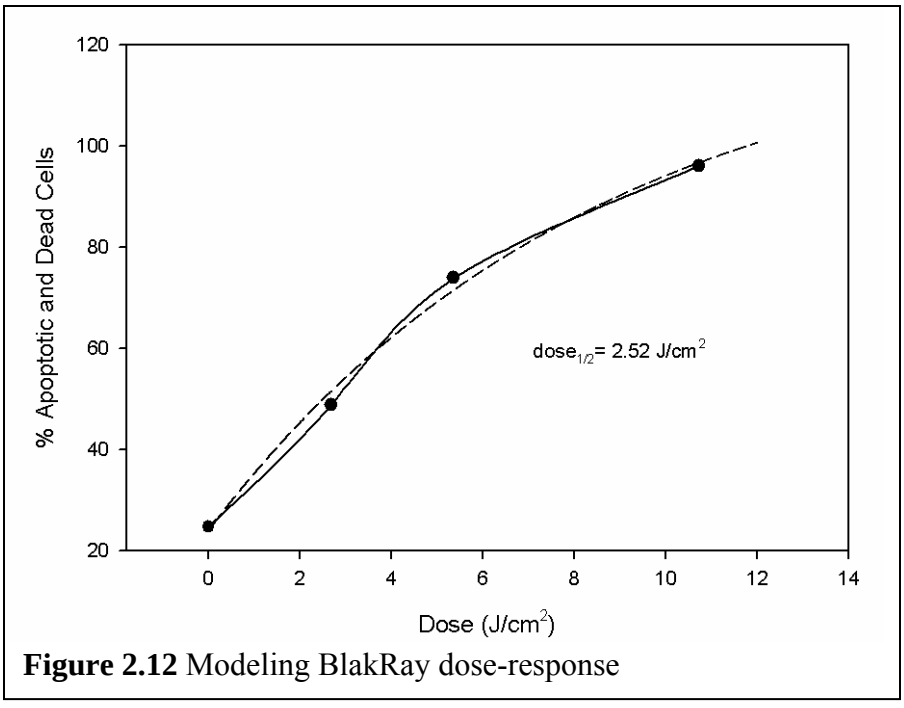

Figure 2.12 Modeling BlakRay dose-response

Effect of Cooling on Photoactivation

Results of cooling-assisted photoactivation are illustrated in Fig. 2.13. The BlakRay alone (5.37 J/cm^2) resulted in 41 ±4.2% dead cells. A significant difference was found when the IR energy was blocked, which resulted in only 24 ±3.3% dead cells. Cells held at the cold plate temperature of 4ºC for the 5.37 J/cm^2 BlakRay light exposure resulted in 23 ±1.5% dead, which is a significant decrease from the BlakRay alone case ($p \leq 0.05$, Student's t-test). No significant difference was observed for the GreenSpot (14.31 J/cm^2) when combined with the cold plate treatment. These results suggest that the BlakRay has some heating associated with exposure that is not seen with the GreenSpot source.

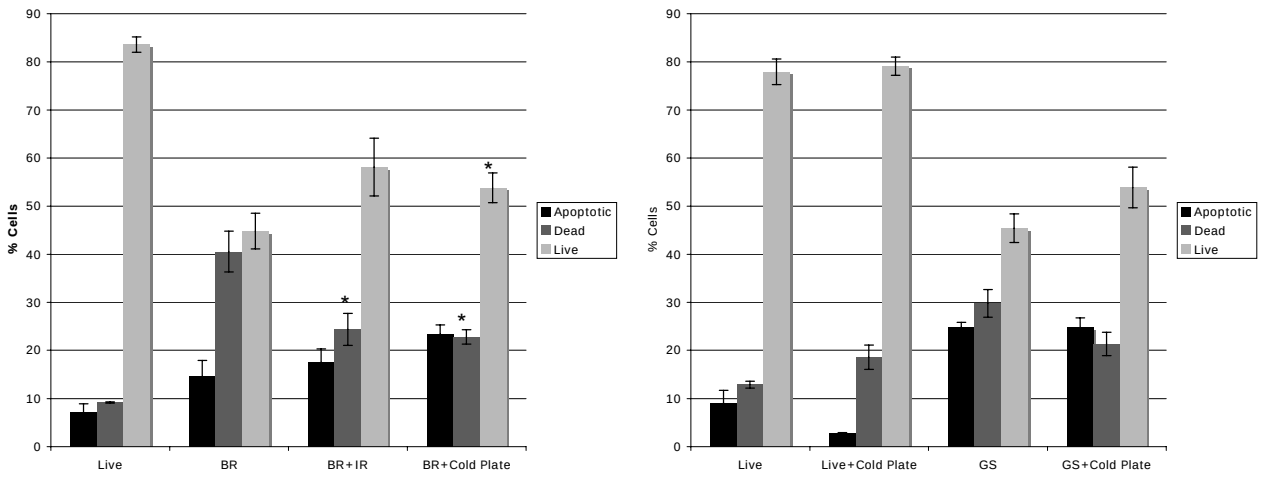

Figure 2.13 Effect of cooling-assisted photoactivation for the BlakRay (BR) (5.37 J/cm^2) and GreenSpot (GS) (14.31 J/cm^2) UVA light sources. ($p \leq 0.05$, Student's t-test)

Photoduration Effects

Differences in the intensity of photoexposure were evaluated for toxicity under similar total doses. Near equivalent GreenSpot doses (6 J/cm^2 and 7.16 J/cm^2) were applied to HeLa cultures, comparing a 20min-GS exposure at a distance of 11.5cm (intensity 5 mW/cm^2) to a

3min-GS exposure at 4.2cm (intensity 39.75 mW/cm^2) as seen in Fig. 2.14. For the 20min-BR exposure with the IR filter, there were 94 ±0.36% apoptotic and dead cells. A significant difference in percentage of apoptotic and dead cells was found for this experiment with 62 ±5% dead and apoptotic for the 20min-GS exposure and 46 ±2.4% for the 3min-GS exposure ($p \leq 0.05$, Student's t-test). These results suggest that the duration of photoexposure could affect the cellular response to UVA.

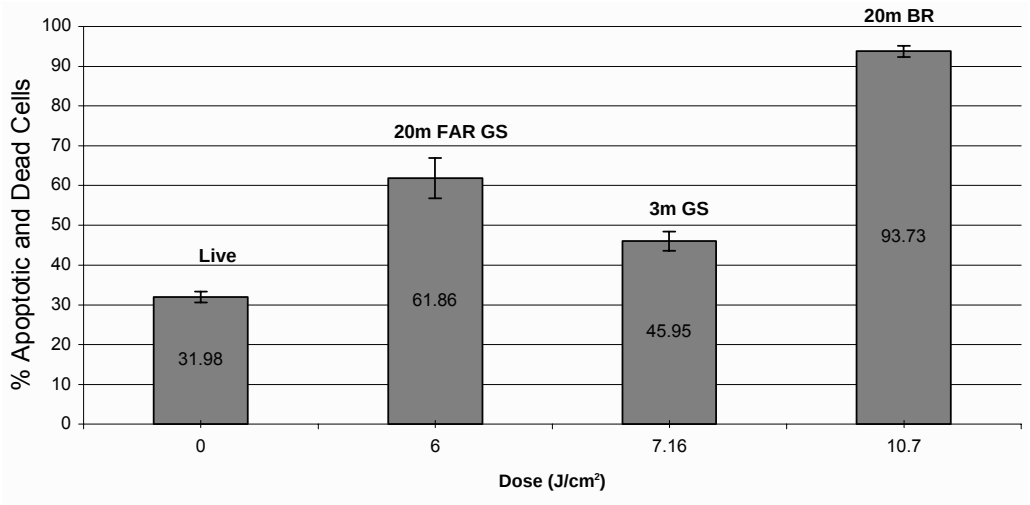

Figure 2.14 Various doses and durations of photoexposure of GS and BR explored the effect of duration of exposure on cell viability.

Discussion

Photoactivating doses were applied to HeLa cells, and apoptosis detection was measured according to an annexin V-Cy5 and propidium iodide apoptosis assay. This study determined the UVA light-induced effects on HeLa cells for two common light sources, which were well-characterized, in terms of spectral output and light intensity. A temperature control and measurement system was used to evaluate the thermal effects resulting from the BR and GS and allow for photoexposures at a controlled temperature of 4°C. Qualitative brightfield phase-

contrast images indicating morphological changes were combined with quantitative flow cytometric data using the annexin V assay to better understand the cellular response of photoactivating doses of UVA.

Several studies have evaluated and commented on the use of the annexin V assay with adherent cells for flow cytometry, applications have included adherent human nonsmall cell lung cancer cells (MR65) and human breast adenocarcinoma (MCF-7) cells (vanEngeland, Ramaekers et al., 1996; Del Bino, Darzynkiewicz et al., 1999). Based on the flow cytometry dotplots in Fig. 2.7, the annexin V assay was successfully able to discriminate distinct live from apoptotic and necrotic cell populations in adherent HeLa cells. Optimization of the timing and assay protocol varies depending on cell type of interest (Willingham 1999).

Initial cell seeding density was found to significantly alter the viability of the live control cells used in the annexin V apoptosis assay. Studies on UVC-induced apoptosis in primary fibroblasts reported decreased levels of apoptosis in confluent cells (Carvalho, da Costa et al., 2003). Other investigators have stressed the importance of cell density in apoptosis experiments (Kvam and Tyrrell 1997; Dahle, Steen et al., 1999).

The UVA threshold for HeLa cells during photoactivation is based on the $dose_{1/2}$ and is useful for establishing the appropriate dose, conditions, and light source to be applied in photoactivation studies. The range of UVA doses (0 - 23.85J/cm^2) used in this study overlap with exposures reported in literature (Shindo and Hashimoto 1997; Zigman, McDaniel et al., 2000). An exponential relationship is seen between the percent of dead and apoptotic cells and increasing light doses, with a $dose_{1/2}$ of 7.6 J/cm^2 on the GreenSpot and 2.52 J/cm^2 on the BlakRay. UVA photoactivation studies employing HeLa cells that exceed this dose are likely to inhibit normal cell function and should be avoided for long-term studies requiring resumption of cell health.

The discrepancy in UVA $dose_{1/2}$ for the two UVA light sources suggests that the intensity of the light source and/or duration of photoexposure affects cell health. The study of similar total GS doses for different photodurations (3 minute vs. 20 minute) resulted in significant differences in percentage of dead and apoptotic cells (Fig. 2.14). These results appear to defy the reciprocity rule which states that a photochemical reaction is directly proportional to the total energy dose, independent of the dose distribution and has been recently supported by others (Merwald, Klosner et al., 2005).

In summary, our data indicate a higher intensity light source for the shortest duration with minimal temperature change is optimal for UVA photoexposure of HeLa cells. No significant difference in cell health was found for the UVA dose of 1.6 J/cm^2 using the GreenSpot light source. Qualitative phase contrast microscopy imaging of morphological changes and quantitative flow cytometric methods indicate that the GreenSpot is far less damaging than the BlakRay, thus a higher intensity UVA exposure for the minimal duration is accomplished. This study is applicable to all UVA photoactivation studies, including caging and photobleaching methods. Application of the UVA threshold for HeLa cells is applicable for minimizing cellular effects that occur during photoactivation studies.

Chapter 3

Conclusions and Future Considerations

Conclusions

The effects of UVA light on cell culture are important for photoactivation studies. The purpose of this study was to determine the UVA light threshold for photoactivating HeLa cells, thus allowing for temporal and spatial control of target molecules without damaging cellular function. In order to study the cellular response of cells to UVA, it was essential that the light sources be well-characterized in terms of spectral output and irradiance. Several sources have noted the confusion of interpreting results from studies that do not describe the UV sources (exact spectrum and dosimetry measurements) thoroughly (Meunier, Sarasin et al., 2002; Trautinger 2003). Here we have compiled data from several UVA and UVB studies in order to compare equivalent doses, irradiances, and post-exposure times. In this study, two light sources were compared, and filters were used to select for the 365nm wavelength of interest and attenuate any infrared that could contribute to direct heating of the cells in the dish. The spectral and power measurements of each light source were essential to finding the GreenSpot and BlakRay UVA dose-response curves.

In an effort to gain more information on the light sources, the thermal effects of each light was measured by monitoring the temperature of cell culture media in a cell dish during a 20-minute light exposure for each light source at room temperature and 4°C. The IR filter did not appear to remove all of the heat during the BlakRay photoexposure, which could possibly result from proximity of the cell dish to the light source. However, the cell media temperature increase for the GreenSpot was 1.5°C less, which was most likely attributed to the physical light apparatus in which the GreenSpot was delivered by an optical fiber, thus eliminating the

proximity to the light source as a concern. The effect of cooling on photoactivation was found to have a significant effect on the BlakRay exposure, which is not surprising due to the thermal effects observed. However, there was no significant effect from cooling during photoactivation with the GreenSpot.

We have demonstrated that the annexin V apoptosis assay can be applied to adherent HeLa cells and used for flow cytometric analysis. The morphological changes of the UVA-irradiated cells were in agreement with the large blebs that have been described by others using light microscopy (Malorni, Donelli et al., 1994). Use of the annexin V-Cy5 and Propidium Iodide apoptosis assay detected changes in live, dead, and apoptotic cell populations by flow cytometry, providing information necessary for determining a UVA dose-response. The literature review concerning the use of the annexin V apoptosis assay with adherent cells indicates mixed results depending on cell type used (vanEngeland, Ramaekers et al., 1996; Del Bino, Darzynkiewicz et al., 1999).

Cell density was found to be significant for studying the mode of cell death for confluent cells and microcolonies according to Dahle, Steen, et al. (1999). By extrapolating this information, we confirmed that cell confluence also affected HeLa cell sensitivity to UVA light. Cells at lower densities are more susceptible to photo-induced damage.

From the flow cytometry data collected, we found that the GreenSpot light source is far less damaging to cells than the BlakRay. By modeling the GS dose-response, we were able to show that UVA doses less than 1.6 J/cm^2 on the GreenSpot show no significant response and the dose$_{1/2}$ is 7.60 J/cm^2. The GreenSpot light source was determined as the UVA light source of choice for photoactivation apoptosis studies with HeLa cells. Therefore, this study provides a basis for conducting photoactivation application experiments on HeLa cells, as long as the UVA light required for photoactivation is less than the determined UVA threshold.

Future Considerations

The project findings presented here allow for an increased understanding of factors to consider when performing UVA photoactivation studies. The annexin V-Cy5/PI assay protocol can differ depending on cell type, making the selection of a cell system to be studied very important. Since an assortment of light sources exists in photobiology literature, the data is difficult to compare and interpret when applying UVA doses to other applications. It is important to acquire a detailed knowledge of the exact spectrum and irradiance of the lamp that is going to be used for photoactivation.

Further studies that apply the GFP assay described previously with the apoptosis assay used here may provide insight into whether the UVA-induced decrease in GFP expression is correlated with induction of apoptosis. The GFP assay could find very different results based on the use of a different 365nm light source, the GreenSpot instead of the BlakRay. Combining GFP with apoptosis could help to identify the molecular effects occurring at the cellular level, which are causing decreased GFP expression with increasing light exposure. To date, the annexin V-Cy5 apoptosis assay has not been combined with a cellular GFP system. The assay we have optimized will work well for simultaneous assessment of GFP expression and apoptosis (using Cy5 and PI) with triply labeled cells using flow cytometry due to the lack of emission overlap from the fluorophores. Cell viability effects resulting from the released cage group for uncaging studies could also be considered. Increased knowledge explaining the decrease in GFP expression could result in improved applications of UVA light to photoactivation techniques in cells.

Initial studies shown in chapter 2 showed that the GreenSpot is the preferred light source for photoexposure with HeLa cells. Future studies exploring the optimal pulse duration for photoactivation could be determined with continuous and fractionated UVA light exposure on

cells (Appendix C). Preliminary data suggest that the effect of various durations (5sec, 10sec, 30sec, 3min, 5min) of the same total dose (3.6 J/cm^2) using a more intense GreenSpot system (irradiance of 0.705 W/cm^2 compared to the 39.75 mW/cm^2 used in the studies in chapter 2) did not find large variation in the percentage of apoptotic and dead cells (Fig. 3.1).

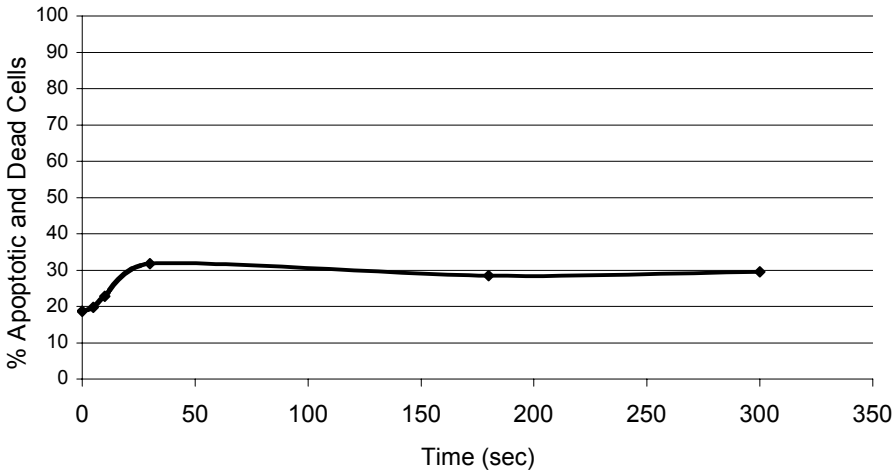

Figure 3.1 Effect of photoduration on cell viability (n=1)

Previously reported studies of photosensitized injury have compared a continuous and pulsed wave UV light source for photosensitization studies on cell culture (Shea, Hefetz et al., 1990). The principle of reciprocity applies in continuous wave and pulsed wave experiments where the injury is proportional to the cumulative radiant exposure (energy incident/unit area) and is independent of irradiance (power incident/unit area) over several orders of magnitude although this could be affected by long durations of exposure. Additional parameters explored for UVA include bulk heating and mitochondrial injury as photobiological events that have been evaluated (Shea, Hefetz et al., 1990).

Use of additional apoptosis assays, such as caspase-3 or mitochondria injury assays, could be used to look at other quantitative apoptosis markers for evaluating the effect of apoptosis due to UVA (Guhl, Hartmann et al., 2003). Improved apoptosis assays optimized for

adherent cells would be of great benefit for studies that quantitatively evaluate apoptosis of adherent cell lines. Application of the annexin V-Cy5/PI assay with a suspension cell line, such as Jurkat cells, could prove as an interesting aside by evaluating if there is a difference in UVA sensitivity for adherent and suspension cells.

In order to study the UVA effects on HeLa cells in more depth, oxidative damage and heat shock protein (hsp) upregulation could also be monitored. UV radiation is a stress factor that is known to cause oxidative damage, which triggers hsp induction (Trautinger 2003). The effects of UVA on hsp's have not been as thoroughly investigated as UVB and UVC, and hsp72 and heme oxygenase-1 (HO-1) are important proteins that UVA irradiation induces (Trautinger 2003). The use of heat shock proteins could also confirm the optimal conditions (temperature and duration) and light source for photoactivating studies in cells. Ultimately, all of these parameters are important for optimizing photobiological research.

References

Aragane, Y., D. Kulms, D. Metze, G. Wilkes, B. Poppelmann, T. A. Luger and T. Schwarz (1998). "Ultraviolet light induces apoptosis via direct activation of CD95 (Fas/APO-1) independently of its ligand CD95L." Journal of Cell Biology **140**(1): 171-182.

Becker, W., L. Kleinsmith and J. Hardin (2003). The World of the Cell. San Francisco, CA, Benjamin-Cummings Publishing Company (Pearson Education).

Brathen, M., H. Banrud, K. Berg and J. Moan (2000). "Induction of multinucleated cells caused by UVA exposure in different stages of the cell cycle." Photochemistry and Photobiology **71**(5): 620-626.

Breuckmann, F., G. von Kobyletzki, A. Avermaete, M. Radenhausen, S. Hoxtermann, C. Pieck, P. Schoneborn, T. Gambichler, M. Freitag, K. Hoffmann and P. Altmeyer (2003). "Mechanisms of apoptosis: UVA1-induced immediate and UVB-induced delayed apoptosis in human T cells in vitro." Journal of the European Academy of Dermatology and Venereology **17**(4): 418-429.

Broitman, S. L., O. Amosova and J. R. Fresco (2003). "Repairing the Sickle Cell mutation. III. Effect of irradiation wavelength on the specificity and type of photoproduct formed by a 3 '-terminal psoralen on a third strand directed to the mutant base pair." Nucleic Acids Research **31**(16): 4682-4688.

Carvalho, H., R. M. A. da Costa, V. Chigancas, R. Weinlich, G. Brumatti, G. P. Amarante-Mendes, A. Sarasin and C. F. M. Menck (2003). "Effect of cell confluence on ultraviolet light apoptotic responses in DNA repair deficient cells." Mutation Research-Reviews in Mutation Research **544**(2-3): 159-166.

Chan, S. D. H., G. Luedke, M. Valer, C. Buhlmann and T. Preckel (2003). "Cytometric analysis of protein expression and apoptosis in human primary cells with a novel microfluidic chip-based system." Cytometry Part A **55A**(2): 119-125.

Dahle, J., H. B. Steen and J. Moan (1999). "The mode of cell death induced by photodynamic treatment depends on cell density." Photochemistry and Photobiology **70**(3): 363-367.

Del Bino, G., Z. Darzynkiewicz, C. Degraef, R. Mosselmans, D. Fokan and P. Galand (1999). "Comparison of methods based on annexin-V binding, DNA content or TUNEL for evaluating cell death in HL-60 and adherent MCF-7 cells." Cell Prolif **32**(1): 25-37.

Giacomoni, P. U. (1995). "Open Questions in Photobiology .2. Induction of Nicks by Uv-A." Journal of Photochemistry and Photobiology B-Biology **29**(1): 83-85.

Godar, D. E. (1999). "Light and death: Photons and apoptosis." Journal of Investigative Dermatology Symposium Proceedings **4**(1): 17-23.

Griffiths, A. D. and D. S. Tawfik (2003). "Directed evolution of an extremely fast phosphotriesterase by in vitro compartmentalization." Embo Journal **22**(1): 24-35.

Guhl, S., K. Hartmann, S. Tapkenhinrichs, A. Smorodchenko, A. Grutzkau, B. M. Henz and T. Zuberbier (2003). "Ultraviolet irradiation induces apoptosis in human immature, but not in skin mast cells." Journal of Investigative Dermatology **121**(4): 837-844.

He, Y. Y., J. L. Huang, R. H. Sik, J. Liu, M. P. Waalkes and C. F. Chignell (2004). "Expression profiling of human keratinocyte response to ultraviolet A: Implications in apoptosis." Journal of Investigative Dermatology **122**(2): 533-543.

Henseleit, U., T. Rosenbach and G. Kolde (1996). "Induction of apoptosis in human HaCaT keratinocytes." Archives of Dermatological Research **288**(11): 676-683.

Isoherranen, K., I. Sauroja, C. Jansen and K. Punnonen (1999). "UV irradiation induces downregulation of bcl-2 expression in vitro and in vivo." Archives of Dermatological Research **291**(4): 212-216.

Kaplan, J. H., B. Forbush and J. F. Hoffman (1978). "Rapid Photolytic Release of Adenosine 5'-Triphosphate from a Protected Analog - Utilization by Na-K Pump of Human Red Blood-Cell Ghosts." Biochemistry **17**(10): 1929-1935.

Kerr, J. F. R., A. H. Wyllie and A. R. Currie (1972). "Apoptosis - Basic Biological Phenomenon with Wide-Ranging Implications in Tissue Kinetics." British Journal of Cancer **26**(4): 239-257.

Koopman, G., C. P. M. Reutelingsperger, G. A. M. Kuijten, R. M. J. Keehnen, S. T. Pals and M. H. J. Vanoers (1994). "Annexin-V for Flow Cytometric Detection of Phosphatidylserine Expression on B-Cells Undergoing Apoptosis." Blood **84**(5): 1415-1420.

Kulms, D., H. Dussmann, B. Poppelmann, S. Stander, A. Schwarz and T. Schwarz (2002). "Apoptosis induced by disruption of the actin cytoskeleton is mediated via activation of CD95 (Fas/APO-1)." Cell Death and Differentiation **9**(6): 598-608.

Kulms, D., B. Poppelmann and T. Schwarz (2000). "Ultraviolet radiation-induced interleukin 6 release in HeLa cells is mediated via membrane events in a DNA damage-independent way." Journal of Biological Chemistry **275**(20): 15060-15066.

Kulms, D., B. Poppelmann, D. Yarosh, T. A. Luger, J. Krutmann and T. Schwarz (1999). "Nuclear and cell membrane effects contribute independently to the induction of apoptosis in human cells exposed to UVB radiation." Proceedings of the National Academy of Sciences of the United States of America **96**(14): 7974-7979.

Kulms, D. and T. Schwarz (2002). "20 years after - Milestones in molecular photobiology." Journal of Investigative Dermatology Symposium Proceedings **7**(1): 46-50.

Kvam, E. and R. M. Tyrrell (1997). "Induction of oxidative DNA base damage in human skin cells by UV and near visible radiation." Carcinogenesis **18**(12): 2379-84.

Leite, M., M. Quinta-Costa, P. S. Leite and J. E. Guimaraes (1999). "Critical evaluation of techniques to detect and measure cell death - study in a model of UV radiation of the leukaemic cell line HL60." Analytical Cellular Pathology **19**(3-4): 139-151.

Lippincott-Schwartz, J., N. Altan-Bonnet and G. H. Patterson (2003). "Photobleaching and photoactivation: following protein dynamics in living cells." Nature Cell Biology: S7-S14.

Malorni, W., G. Donelli, E. Straface, M. T. Santini, S. Paradisi and P. U. Giacomoni (1994). "Both Uva and Uvb Induce Cytoskeleton-Dependent Surface Blebbing in Epidermoid Cells." Journal of Photochemistry and Photobiology B-Biology **26**(3): 265-270.

Merwald, H., G. Klosner, C. Kokesch, M. Der-Petrossian, H. Honigsmann and F. Trautinger (2005). "UVA-induced oxidative damage and cytotoxicity depend on the mode of exposure." J Photochem Photobiol B **79**(3): 197-207.

Meunier, J. R., A. Sarasin and L. Marrot (2002). "Photogenotoxicity of mammalian cells: A review of the different assays for in vitro testing." Photochemistry and Photobiology **75**(5): 437-447.

Monroe, W. T., M. M. McQuain, M. S. Chang, J. S. Alexander and F. R. Haselton (1999). "Targeting expression with light using caged DNA." Journal of Biological Chemistry **274**(30): 20895-20900.

Patton, W. F., J. S. Alexander, A. B. Dodge, R. J. Patton, H. B. Hechtman and D. Shepro (1991). "Mercury-Arc Photolysis - a Method for Examining 2nd Messenger Regulation of Endothelial-Cell Monolayer Integrity." Analytical Biochemistry **196**(1): 31-38.

Pourzand, C. and R. M. Tyrrell (1999). "Apoptosis, the role of oxidative stress and the example of solar UV radiation." Photochemistry and Photobiology **70**(4): 380-390.

Rosette, C. and M. Karin (1996). "Ultraviolet light and osmotic stress: Activation of the JNK cascade through multiple growth factor and cytokine receptors." Science **274**(5290): 1194-1197.

Schindl, A., G. Klosner, H. Honigsmann, G. Jori, P. C. Calzavara-Pinton and F. Trautinger (1998). "Flow cytometric quantification of UV-induced cell death in a human squamous cell carcinoma-derived cell line: dose and kinetic studies." Journal of Photochemistry and Photobiology B-Biology **44**(2): 97-106.

Shea, C. R., Y. Hefetz, R. Gillies, J. Wimberly, G. Dalickas and T. Hasan (1990). "Mechanistic Investigation of Doxycycline Photosensitization by Picosecond-Pulsed and Continuous Wave Laser Irradiation of Cells in Culture." Journal of Biological Chemistry **265**(11): 5977-5982.

Shindo, Y. and T. Hashimoto (1997). "Time course of changes in antioxidant enzymes in human skin fibroblasts after UVA irradiation." Journal of Dermatological Science **14**(3): 225-232.

Trautinger, F. (2003). Stress Proteins in the Photobiology of Mammalian Skin. Handbook of Photochemistry and Photobiology. H. S. Nalwa. Stevenson Ranch, American Scientific Publishers. **4 (Photobiology):** 149-158.

Tyrrell, R. M. and S. M. Keyse (1990). "New Trends in Photobiology - the Interaction of Uva Radiation with Cultured-Cells." Journal of Photochemistry and Photobiology B-Biology **4**(4): 349-361.

van Engeland, M., L. J. W. Nieland, F. C. S. Ramaekers, B. Schutte and C. P. M. Reutelingsperger (1998). "Annexin V-affinity assay: A review on an apoptosis detection system based on phosphatidylserine exposure." Cytometry **31**(1): 1-9.

vanEngeland, M., F. C. S. Ramaekers, B. Schutte and C. P. M. Reutelingsperger (1996). "A novel assay to measure loss of plasma membrane asymmetry during apoptosis of adherent cells in culture." Cytometry **24**(2): 131-139.

Willingham, M. C. (1999). "Cytochemical methods for the detection of apoptosis." Journal of Histochemistry & Cytochemistry **47**(9): 1101-1109.

Yao, R. Y. and C. B. Wang (2002). "Protective effects of polypeptide from Chlamys farreri on Hela cells damaged by ultraviolet A." Acta Pharmacologica Sinica **23**(11): 1018-1022.

Zigman, S., T. McDaniel, J. Schultz and J. Reddan (2000). "Effects of intermittent UVA exposure on cultured lens epithelial cells." Current Eye Research **20**(2): 95-100.

Appendix A: Annexin V-Cy5, PI Apoptosis Assay Protocol

A. Observe and take brightfield images of cells seeded in 35mm dishes within 18 hrs of photoexposure treatments

B. Harvest cells

1) Keep floaters (1.25 mL) in 5mL Falcon flow cytometry tubes
2) Wash 0.75 mL PBS and Keep 1st wash
3) Rinse 0.75 mL PBS and discard
4) Add 1 mL 0.25% trypsin. Allow 5-7 minutes for cells to detach from the bottom of the dish.
5) Add 1 mL of DMEM-RS (+3% FBS)
6) Transfer cells in solution to 5 mL cytometer tube
7) Spin down at 500g's for 5minutes
8) Aspirate carefully using 1 mL pipettor

C. Wash procedure

1) Resuspend the cells in 200 μL DMEM-RS
2) Spin down at 500g's for 5minutes
3) Aspirate carefully using 1 mL pipettor

D. Stain (Staining steps are done under the hood with the light off)

1) Add 200 μL 1x Binding Buffer (MBL Annexin V-Cy5 kit)
    i. Add 4 μL Annexin V-Cy5
    ii. Add 6 μL Propidium Iodide (Note: Double glove when using PI, and dispose of PI tips appropriately)
2) Keep tubes protected from light
3) Vortex gently and allow cells to incubate for 15-20 minutes covered in the dark at room temperature
4) Spin down at 500g's for 5minutes
5) Aspirate carefully using 1 mL pipettor
6) Add 100 μL PBS (with Calcium and Magnesium) to each tube for flow cytometry

E. Run flow cytometry at Veterinary Medicine

1) Take labeled sheet and numbered tubes to Vet Med with cell sample tubes covered in foil and on ice

Appendix B: Basic Stamp Program for Thermocouple Kit

```
'   {$STAMP BS2p, KTablePos.BPE, JTablePos.BPE, TTablePos.BPE}
'   {$PBASIC 2.5}
'   {$PORT COM1}

'Setup serial communications for stampDAQ
sPin   CON   16   'Serial Pin - P16, Programming port
Baud   CON   240  'Baud mode for a rate of 9600, 8-N-1

' -----[ I/O Definitions ]---------------------------------------------

OW            PIN     8                 ' 1-Wire buss pin


' -----[ Constants ]-----------------------------------------------------

ReadNet       CON     $33               ' read OW net address
SkipNet       CON     $CC               ' skip OW net address
RdReg         CON     $69               ' read register
MatchNet      CON     $55               ' match address
SearchNet     CON     $F0               ' search net address


' -----[ Variables ]-----------------------------------------------------

vIn           VAR     Word              ' in millivolts
tmpCJ         VAR     Word              ' device temp in C
tCuV          VAR     Word              ' thermocouple millivolts
sign          VAR     Byte              ' TC sign bit

highComp      VAR     Word
lowComp       VAR     Word

cjComp        VAR     Word              ' temp compensation
tempC         VAR     Word              ' temp in Celsius
temp          VAR     Word              ' variable for interpolating temp

tblLo         VAR     Word              ' table pointers
tblHi         VAR     Word
eePntr        VAR     Word
testVal       VAR     Word              ' test value from table
error         VAR     Bit               ' 1 = out of range
device        VAR     Bit               ' device 0 or 1?

PAUSE 1000    'Allow data communications to stabilize
```

```
SEROUT sPin,Baud,[CR]   'Send a lone CR to ensure StampDAQ buffer is ready

STORE 2      'load table pointer

'*********************************************************
Configure:

SEROUT sPin,Baud,[CR,"LABEL,TIME,TEMPC_0,TEMPC_1",CR]  'Label 3 columns

SEROUT sPin,Baud,["CLEARDATA",CR]    'Clear all data columns (A-J) in Excel

'*****************************************  GET ROM ID's for thermocouple units


Main:
  a_loop:
     'get temperature from device 0
     device = 0
     GOSUB readTemp
     'Send String with data for Excel
     temp = ((100*tempC.LOWBYTE)/256)
     SEROUT sPin,Baud,["DATA,TIME",",",DEC tempC.HIGHBYTE,".",DEC temp,","]


     'get temperature from device 1
     device = 1
     GOSUB readTemp
     'Send String with data for Excel
     temp = ((100*tempC.LOWBYTE)/256)
     SEROUT sPin,Baud,[DEC tempC.HIGHBYTE,".",DEC temp,",",CR]

     PAUSE 875    '1 second wait before starting again
  GOTO a_loop
  STOP

'***************************************** get temp

readTemp:
   GOSUB Read_TC_Volts                                  ' read Seebeck voltage
   GOSUB Read_CJ_Temp                                   ' read cold junction temp
   READ (2 * tmpCJ.HIGHBYTE), Word lowComp       ' lowest compensation temp for
interpolation
   READ (2 * tmpCJ.HIGHBYTE + 2), Word highComp                 ' highest compensation
value
   cjComp = lowComp + ((highComp-lowComp) */ tmpCJ.LOWBYTE)        'linear interpolate
```

```
    ' combine cjComp and tCuV
    '
    IF sign THEN
      ' TC below cold junction
      IF (tCuV < cjComp) THEN
        cjComp = cjComp - tCuV
      ELSE
        cjComp = 0                      ' limit to 0C
      ENDIF
    ELSE
      ' TC above cold junction
      cjComp = cjComp + tCuV
    ENDIF

    tblHi = 1023                        ' set high end of search
    GOSUB TC_Lookup                     ' reverse lookup of table
  RETURN

'****************************************** temp functions

' Reads device input voltage (Vin pin)
' -- mV in millivolts (max reading is 4.75 volts)

Read_Vin:
  IF DEVICE THEN
    OWOUT OW, %0001, [MatchNet, $30,$B0,$3E,$05,$10,$00,$00,$FE,  RdReg, $0C]
  ELSE
    OWOUT OW, %0001, [MatchNet, $30,$6A,$54,$05,$10,$00,$00,$59,  RdReg, $0C]
  ENDIF
  OWIN  OW, %0010, [vIn.BYTE1, vIn.BYTE0]
  IF (vIn.BIT15) THEN                   ' check sign
    vIn = 0                             ' disallow negative
  ELSE
    vIn = vIn >> 5 */ $4E1              ' x 4.88 millivolts
  ENDIF
  RETURN


' Reads current register to get TC voltage
' -- each raw bit = 15.625 uV
' -- tCuV in microvolts

Read_TC_Volts:
  'OWOUT OW, %0001, [SkipNet, RdReg, $0E]        ' read current register
  IF DEVICE  THEN
    OWOUT OW, %0001, [MatchNet, $30,$B0,$3E,$05,$10,$00,$00,$FE,  RdReg, $0E]
  ELSE
```

```
  OWOUT OW, %0001, [MatchNet, $30,$6A,$54,$05,$10,$00,$00,$59,  RdReg, $0E]
 ENDIF
 OWIN  OW, %0010, [tCuV.BYTE1, tCuV.BYTE0]
 sign = tCuV.BIT15                  ' save sign bit
 tCuV = tCuV >> 3                   ' correct alignment
 IF sign THEN
  tCuV = tCuV | $F000               ' pad 2's-compliment bits
 ENDIF
 tCuV = ABS tCuV */ 4000            ' x 15.625 uV     0x0FA0
 RETURN

' Reads cold junction (device) temperature
' -- each raw bit = 0.125 degrees C
' -- returns tmpCJ in whole degrees C

Read_CJ_Temp:
 'OWOUT OW, %0001, [SkipNet, RdReg, $18]
 IF DEVICE  THEN
  OWOUT OW, %0001, [MatchNet, $30,$B0,$3E,$05,$10,$00,$00,$FE,  RdReg, $18]
 ELSE
  OWOUT OW, %0001, [MatchNet, $30,$6A,$54,$05,$10,$00,$00,$59,  RdReg, $18]
 ENDIF
 OWIN  OW, %0010, [tmpCJ.BYTE1, tmpCJ.BYTE0]
 IF (tmpCJ.BIT15) THEN              ' check sign
  tmpCJ = 0                         ' disallow negative
 ELSE
  tmpCJ.HIGHBYTE = tmpCJ.HIGHBYTE
  tmpCJ.LOWBYTE = tmpCJ.LOWBYTE & $E0
 ENDIF
 RETURN

'Search currently selected TC table FOR nearest entry
' -- uses modified binary algorithm to find cjComp
' -- high end of search set before calling (tblHi)
' -- successful search sets tempC

TC_Lookup:
 tblLo = 0                          ' low entry of table
 tempC = 22                         ' default to room temp

 READ (tblHi * 2), Word testVal     ' check max temp
 IF (cjComp > testVal) THEN
  error = 1                         ' out of range
 ELSE
  DO
   eePntr = (tblLo + tblHi) / 2     ' midpoint of search span
   READ (eePntr * 2), Word testVal   ' read value from midpoint
```

```
    IF (cjComp = testVal) THEN
      EXIT                              ' found it!
    ELSEIF (cjComp < testVal) THEN
      tblHi = eePntr                    ' search lower half
    ELSE
      tblLo = eePntr                    ' search upper half
    ENDIF

    IF ((tblHi - tblLo) < 2) THEN       ' span at minimum
      eePntr = tblLo
      EXIT
    ENDIF
  LOOP

  READ (eePntr * 2), Word testVal  'interpolate between table values
  READ (eePntr * 2 + 2), Word temp
  tempC.HIGHBYTE = eePntr
  tempC.LOWBYTE = (256*(cjComp-testVal))/(temp - testVal)
ENDIF
RETURN


' =============================================================================
'
'   File..... JTablePos.BPE
'   Purpose... J-type (Iron/Constantan) thermocouple data (0C reference)
'   Author.... Compiled by Parallax
'   E-mail.... support@parallax.com
'   Started...
'   Updated... 19 JAN 2004
'
'   {$STAMP BS2p}
'   {$PBASIC 2.5}
'
' =============================================================================
```

Appendix C: Programmable Logic Control: Pulsed GreenSpot

Programmable logic control via an RCA jack (phono connector) located on the back of the unit has been instrumented with a relay and basic stamp microcontroller to run accurate, repeatable, and easily measurable fractionated light exposures (Fig. A.C.1).

```
' {$STAMP BS1}

MAIN:
  HIGH 7
  PAUSE 500
  LOW 7
  PAUSE 500
GOTO MAIN
```

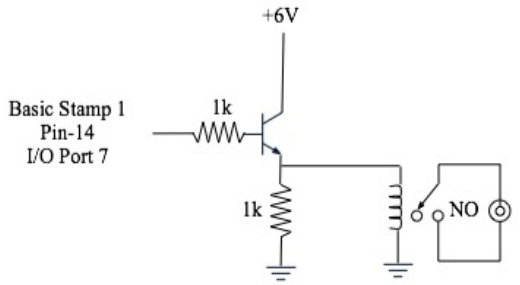

Figure A.C.1. GreenSpot PLC wiring diagram for basic stamp microcontroller, relay, and RCA jack.

Appendix D: Staurosporine Dose, Post-Exposure Time

Preliminary experiments were conducted at various staurosporine doses and post-exposure times for HeLa cells to determine the optimal chemically-induced apoptotic control as shown in Fig. A.D.1).

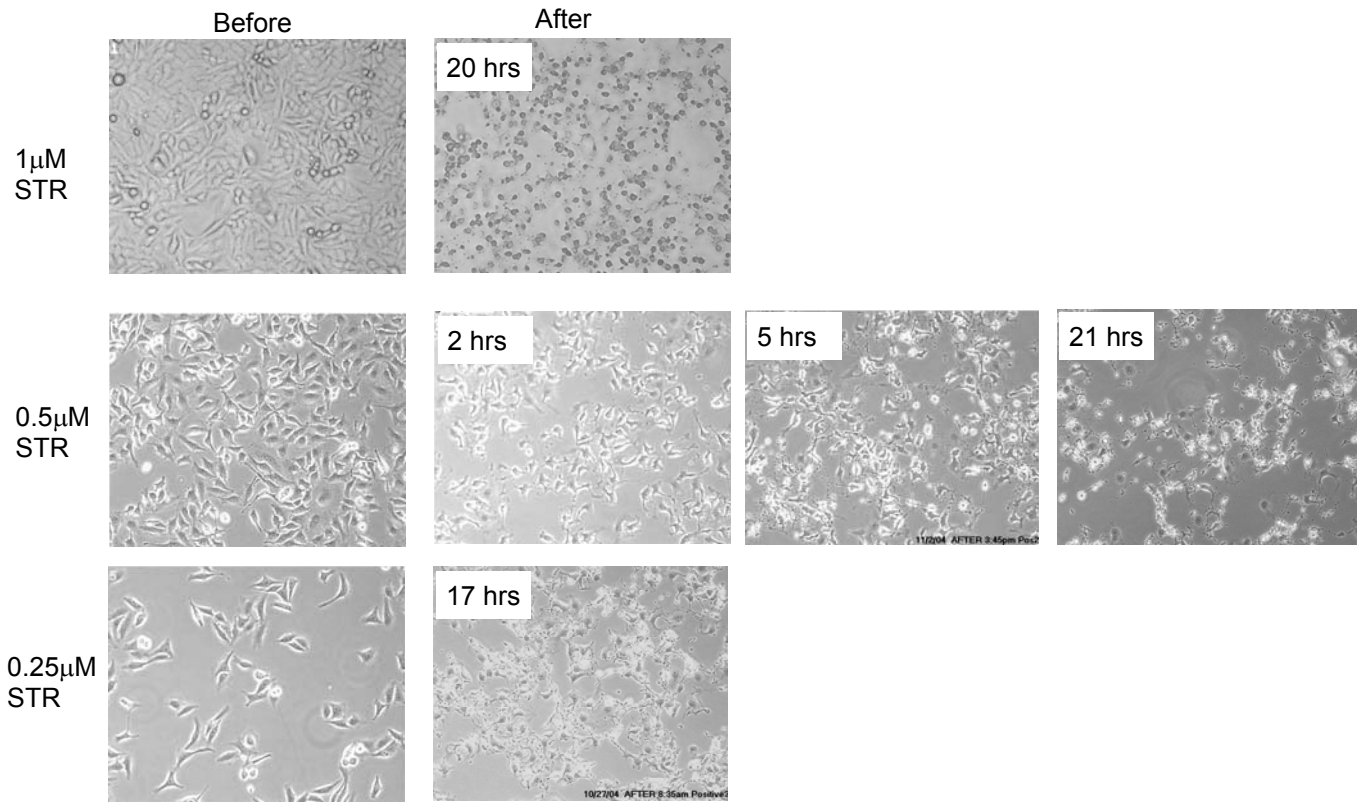

Figure A.D.1. To improve the apoptotic control cell population, staurosporine (STR) doses were varied to find the optimal dose of staurosporine and time post-exposure to induce apoptosis in HeLa cells.

Vita

Julianne Marie Forman was born in Baton Rouge, Louisiana, on May 1, 1980. She remained in Baton Rouge where she grew up. Julianne attended Louisiana Tech University in biomedical engineering in the fall of 1998 and later transferred to Louisiana State University in the spring of 2000. She finished her bachelor's degree in 2002 in biological and agricultural engineering at Louisiana State University. After working in graduate school at the University of Kentucky in Lexington, Kentucky, for a semester, Julianne returned to Louisiana State University to pursue a master's degree in biological and agricultural engineering.